Title
Deletion of the imprinted gene, Grb10, promotes hematopoietic stem cell self-renewal and regeneration

Author
Yan, Xiao

Publication Date
2017

Peer reviewed|Thesis/dissertation

UNIVERSITY OF CALIFORNIA

Los Angeles

Deletion of the imprinted gene, Grb10, promotes hematopoietic stem cell self-renewal and regeneration

A dissertation submitted in partial satisfaction of the requirements for the degree Doctor of Philosophy in Molecular and Medical Pharmacology

by

Xiao Yan

2018

ABSTRACT OF THE DISSERTATION

Deletion of the imprinted gene, Grb10, promotes hematopoietic stem cell self-renewal and regeneration

by

Xiao Yan

Doctor of Philosophy in Molecular and Medical Pharmacology

University of California, Los Angeles, 2018

Professor John P. Chute, Co-Chair

Professor Heather R. Christofk, Co-Chair

Imprinted genes have been shown to be differentially expressed by adult stem cells, but the function of imprinted genes in regulating adult stem cell fate is not well understood. Here, we show that growth factor receptor bound protein 10 (Grb10), a member of the imprinted gene family, regulates hematopoietic stem cell (HSC) self-renewal and regeneration. Deletion of the maternal allele of Grb10 in mice ($Grb10^{m/+}$ mice) substantially increased HSC long-term repopulating capacity compared to $Grb10^{+/+}$ mice. Furthermore, following total body irradiation (TBI), $Grb10^{m/+}$ mice displayed accelerated HSC regeneration and overall hematopoietic reconstitution compared to $Grb10^{+/+}$ mice. Grb10-deficient HSCs displayed increased migratory capacity and proliferative capacity in vivo following competitive transplantation or irradiation, commensurate with increased activation of the RhoGTPase, Rac1. Inhibition of Rac1 abrogated

both the enhanced migratory capacity and the increased proliferative potential of Grb10-deficient HSCs in vivo. Grb10 has a long-established role as a negative feedback inhibitor of Akt-mTOR signaling pathway. In accordance with this, our data show that inhibition of Akt-mTOR signaling pathway abolished the early regeneration of long-term HSCs in $Grb10^{m/+}$ mice following irradiation, compared to $Grb10^{+/+}$ mice. This study reveals a previously unrecognized role for the imprinted gene, Grb10, in regulating HSC self-renewal and regeneration and suggests that antagonism of Grb10 can promote hematopoietic regeneration in vivo.

The dissertation of Xiao Yan is approved.

Steven M. Dubinett

Michael E. Jung

Heather R, Christofk, Committee Co-Chair

John P. Chute, Committee Co-Chair

University of California, Los Angeles

2018

Table of Contents

List of Figures

Acknowledgements

I would like to give my sincere gratitude to my advisor Dr. John Chute. His broad knowledge on the basic biology and clinical practice gives me a unique training on the research perspectives. His persistent seeking on novel therapeutic method of irradiation damage motivates me to keep working on drug development during and after PhD study. His endeavor to bring sufficient funding to the lab enables my research project. I could not image finding a better advisor for my PhD.

Besides my advisor, I would also like to express my thanks to the rest of my committee at UCLA: Dr. Heather Christofk, Dr. Steven Dubinett and Dr. Michael Jung. I transferred from Duke University to UCLA at the end of my PhD study, my committee members here kindly agreed to be on my committee shortly after my request, and provided insightful comments and tremendous help on me finishing my degree. I also want to thank Dr. Samson Chow for his help on my transfer and Dr. Jing Huang for her advice. And I want to give my special thanks to my former committee at Duke: Dr. Christopher Newgard, Dr. David Kirsch, Dr. Nelson Chao and Dr. Xiao-fan Wang. For my first four years in graduate school at Duke University, they guide me to become a capable and independent researcher.

I was also fortunate to be working with a group of talented and friendly labmates. Among them, Dr. Heather Himburg, Dr. Phuong Doan and Dr. Mamle Quarmyne are my additional mentors in the lab. And all the rest of my labmates both at Duke University and UCLA are involved in the warm discussion of my project and many of them have performed critical experiments for my paper. I would never be able to publish my project without them.

I want to thank all my friends, not only at Duke University and UCLA, but also those that are in China or elsewhere around the world. I could not achieve what I have today without their influence and help. They show me how to become a good scientist, and most importantly, how to become a good person.

Last but not least, I want to thank my parents and the rest family members in China. They supported me spiritually all the way through my life. And my wife, Dr. Yu Jiang. She kept me company through all the frustrations these years. I am so fortunate to have her by my side.

Abstract, Chapter 2 and 3 are a version of [Xiao Yan, Heather A. Himburg, Katherine Pohl, Mamle Quarmyne, Evelyn Tran, Yurun Zhang, Tiancheng Fang, Jenny Kan, Nelson J. Chao, Liman Zhao, Phuong L. Doan, John P. Chute, Deletion of the Imprinted Gene Grb10 Promotes Hematopoietic Stem Cell Self-Renewal and Regeneration, In Cell Reports, Volume 17, Issue 6, 2016, Pages 1584-1594, ISSN 2211-1247, https://doi.org/10.1016/j.celrep.2016.10.025.]

Vita

EDUCATION

Duke University, Durham NC

Non-degree Program, Pharmacology and Cancer Biology 2010-2014

Peking University, Beijing, China

BS, Biological Science 2010

PROFESSIONAL EXPERIENCE

Researcher, Broad Stem Cell Research Center, UCLA 2014-

Research Assistant, Div. of Cellular Therapy, Duke University 2011-2014

AWARDS & HONORS

- BD Stem Cell Research Grant
- Abstract Achievement Award, American Society of Hematology Annual Meeting
- Abstract Achievement Award, American Society of Hematology Annual Meeting
- UCLA and Duke Scholarships
- President's Undergraduate Research Fellowship
- Founder Scholarships, Suzhou Industrial Park Scholarships

PUBLICATIONS

- Yan, X., Himburg, H., Pohl, K., Quarmyne, M., Tran, E., Zhang, Y., Kan, J., Chao, N., Zhao, L., Doan, P. & Chute, J. Deletion of the imprinted gene, Grb10, promotes hematopoietic stem cell self-renewal and regeneration. *Cell Reports, in revision*.
- Himburg, H., Doan, P., Yan, X., Quarmyne, M., Zhao, L., Tran, E., Chao, N.J.., Harris, J. & Chute, J.P. Dickkopf1 regulates hematopoietic stem cell regeneration. *Nature Medicine, in revision*.
- Quarmyne, M., Doan, P.L., Himburg, H.A., Yan, X., Nakamura, M., Zhao, L., Chao, N.J. & Chute, J.P. Protein tyrosine phosphatase-sigma regulates hematopoietic stem cell-repopulating capacity. *J Clin Invest* **125**, 177-182 (2015).
- Himburg, H.A., Yan, X., Doan, P.L., Quarmyne, M., Micewicz, E., McBride, W., Chao, N.J., Slamon, D.J. & Chute, J.P. Pleiotrophin mediates hematopoietic regeneration via activation of RAS. *J Clin Invest* **124**, 4753-4758 (2014).
- Zheng, L., Yan, X., Suchindran, S., Dressman, H., Chute, J.P. & Lucas, J. Biological pathway selection through Bayesian integrative modeling. *Stat Appl Genet Mol Biol* **13**, 435-457 (2014).

PRESENTATIONS

- Presentation, 13th Annual Meeting of International Society for Stem Cell Research, San Francisco, CA 2016
- Platform Speaker, UCLA-Bayer Pharmaceuticals Drug Development Workshop, Los Angeles, CA 2016
- Presentation, Blood and Marrow Transplantation Tandem Meeting, Honolulu, HI, 2016

Chapter 1 Introduction

1.1 The origin of hematopoietic stem cells

Hematopoietic stem cell (HSC) possesses the unique capacity of self-renewal and differentiation to all lineages in the blood system. In adult mammals, HSCs are rare cells in the bone marrow and give birth to a hierarchy of progenitors and eventually mature blood cells, include erythrocytes, megakaryocytes, monocytes, and lymphocytes[1]. Previous studies have been controversial about the existence of the hemangioblast, a common clonal progenitor for hematopoietic and endothelial cells[2,3]. In mammals, hematopoiesis arises in the aorta-gonad mesonephros (AGM) regions first, then later fetal liver, and eventually bone marrow[2]. Recently the placenta has also been added as an additional hematopoietic organ during fetal period[1]. During the development, HSCs migrate through the hematopoietic compartments and eventually into bone marrow. Among all the cellular factors in the microenvironment, chemokine (C-X-C motif) ligand 12 (CXCL12) and stem cell factor (SCF) have been proven to have key regulatory role for HSC migration[4,5].

1.2 Hierarchy of hematopoietic stem cells

Hematopoietic stem cells differentiate into a variety of cells from long-term stem cells to mature hematopoietic cells that have no self-renewal capability. Cells with "stemness" only represent a very rare population in the bone marrow, the frequency of which is 0.0001%-0.005%, according to previous publications[6,7]. Long-term HSCs (LT-HSCs) are the most primitive stem cell population with unlimited self-renewal capability. The long-term reconstitution capacity can be assessed by transplantation of single cells into lethally irradiated mice and monitor the repopulation of stem cells. Short-term HSCs are derived from LT-HSCs, and they possess

limited capability of self-renewal and will differentiate within 3 to 6 months. ST-HSC further differentiates into multipotent progenitors (MPPs). MPPs have no self-renewal capability, but they still maintain the potential to differentiate into all lineages in the hematopoietic system[8].

Differentiation of MPPs leads to the divergence of lineage-restricted progenitors, common myeloid progenitors (CMP) and common lymphoid progenitors (CLP). Granulocyte-monocyte progenitors (GMPs) and megakaryocyte-erythroid progenitors (MEPs) are further differentiated from CMPs and produce macrophages, neutrophils or megakaryocyte, red blood cells and platelets, respectively[9]. CLPs are limited to produce cells in the immune system, including B and T lymphocytes, and natural killer (NK) cells[10].

Recently studies show that dendritic cells (DCs), can originate from either CMPs or CLPs[11,12]. It is very interesting to point out that both MPPs and CLPs can migrate from bone marrow to the thymus and initiate T cell development[13]. However, the molecular mechanisms that dominate the lineage potential in these migrated MPPs remain unknown. Previous research show that $CCR9^+$ MPPs, one of the MPPs that have lymphoid differentiation trend, is the main MPP migrates to thymus[14]. Notch signaling was shown to play a critical role in the development of T cells, by preventing the production of B cells from these $CCR9^+$ MPPs in the thymus[14]. Further research will need to be conducted to determine the other signaling pathways that are involved in the T cell-oriented differentiation of MPPs.

1.3 Characterization of hematopoietic stem cells

A comprehensive marker system has been established to distinguish different cell population in the hematopoietic lineage. A common method is to enrich HSCs by staining of cell surface markers c-Kit, Sca-1 and Lineage, and selecting for $c\text{-}Kit^+Sca\text{-}1^+lineage^-$ (KSL) cells. However, KSL cells still consist a combination of cells possessing different cell renewal capability. Only

10% of KSL cells have shown to have long-term repopulating capacity in the bone marrow transplantation assay[15]. To further enrich long-term HSCs, two additional markers, CD34 and Flt3, have been utilized to separate KSL cells into KSL $CD34^{-}Flt3^{-}$ long-term HSCs, and KSL $CD34^{+}Flt3^{-}$ short-term HSCs, and KSL $CD34^{+}Flt3^{+}$ cells that are responsible primarily for rapid lymphoid reconstitution[16]. It is of note that recent research has developed a new and more efficient labeling system of HSCs, the signaling lymphocytic activation molecule (SLAM) family of HSC cell surface markers[17]. $CD150^{+}CD48^{-}c\text{-}Kit^{+}Sca\text{-}1^{+}Lineage^{-}$ (SLAM KSL) cells are enriched for HSCs, with one third of which are long-term HSCs. $CD150^{-}CD48^{-}$KSL cells are enriched for multipotent progenitors (MPPs), while common myeloid progenitors (CMPs) can be marked as $CD34^{+}Fc\gamma R^{-}Lineage^{-}Sca1^{-}c\text{-}Kit^{+}$ cells, and common lymphoid progenitors (CLPs) be marked as $Lineage^{-}Sca\text{-}1^{-}c\text{-}Kit^{-}Flt3^{-}IL7R\alpha^{+}$ cells[18]. For the mature cell lineage, B220 is used to mark B-lymphocytes, CD4 and CD8 are used for detection of T lymphocytes, while Mac-1 and Gr-1 are used for myeloid cells and Ter119 for erythroid cells.

Similar to the mouse, human HSCs can be identified by a combination of cell surface markers. The majority of human HSCs can be enriched by positive selection of CD34[19]. Additional markers, including CD45RA[20], Thy1[21] and CD38[22] have been discovered for the further enrichment of human HSCs. In conclusion, human LT-HSCs are enriched in $CD34^{+}CD38^{-}CD45RA^{-}Thy1^{+}$ cells and MPPs can be characterized by $CD34^{+}CD38^{-}CD45RA^{-}Thy1^{-}$ cells. Recently our lab has identified a cell surface marker, protein tyrosine phosphatase receptor type S (PTPRS) that has the potential to serve as an additional marker for human HSCs[23].

1.4 HSC assays

Besides flow cytometry-based phenotypic assays, a set of functional assays has been established to assess hematopoietic cells at different differentiation stage. Progenitors, mainly myeloid

progenitors, can be detected by colony-forming cell (CFC) assay. Cells from bone marrow, cord blood and mobilized peripheral blood are usually used for the CFC assay. Standard CFC assay contains a culture period of 14 days[24]. Different cell populations, including colony-forming units-granulocyte/macrophages (CFU-GM), burst forming units-erythroid (BFU-E) and colony forming units –granulocytes, erythrocytes, macrophages and megakaryocytes (CFU-GEMM) can be distinguished and counted from CFC results. Long-term culture-initiating cell (LTC-IC) assay has been developed to provide a quick method to evaluate HSCs in vitro, although the readout mainly stands for short-term HSCs[25]. Tested cells were co-cultured with a single layer of endothelial cells for 4 weeks and the stem cells were analyzed by colony-forming cell assay. The gold standard assay for HSC biology is the competitive repopulation unit assay (CRU). In this assay, tested bone marrow cells were mixed with competitor cells in a predetermined ratio, and injected through tail vein into lethally irradiated recipient mice. At certain times after bone marrow transplantation, peripheral blood from recipient mice were sampled and stained for donor cell engraftment. To assess the effect of the long-term hematopoietic stem cells, bone marrow cells from primary recipient mice were isolated and injected through tail vein into lethally irradiated recipient mice, which are the secondary recipient mice. Donor engraftment data from secondary recipient mice are indicators of the long-term HSC performance.

1.5 HSC microenvironment

Hematopoietic stem cells are found to reside in stem cell niches----a local tissue microenvironment that provides growth signals and maintains the "stemness" of the stem cells[26]. Previous studies discovered the existence of two different kinds of HSC niches: the endosteal niche near the bone surface and comprised of osteoblasts, and the vascular niche near the sinusoidal vessels[26]. The concept of endosteal niche has been controversial over the years. Notch

signaling, through Notch Ligand Jagged-1, can stimulate more HSCs by regulation of osteoblasts, suggesting a regulatory role of osteoblasts in the hematopoietic stem cell maintenance[27]. However, conditional deletion of CXCL12 or SCF in the osteoblasts have not influenced the normal function of HSCs, either by complete blood counts or bone marrow reconstitution experiments[28,29]. These data suggest that osteoblasts are dispensable for HSC maintenance. However, this can be explained by lack of specific mouse models to knock out osteoblasts.

Extensive studies have been performed to study the role of endothelial cells in the HSC niche. Growth factors, such as CXCL12, epidermal growth factor (EGF), pleiotrophin (PTN), and stem cell factor (SCF), have all been shown to be secreted by endothelial cells and regulate HSC proliferation or retention at homeostasis or in response to stress such as injury[30,31]. Recent study also identified a novel mechanism that endothelial cells support HSC by expression of cell surface markers including E-selectin[32].

Besides endothelial cells, perivascular cells in the HSC niche have recently been discovered to have key functions for HSC maintenance and regeneration. Among all the perivascular cells, CD146 and platelet-derived growth factor receptor-α expressing cells localized near HSCs, and these cells have high expression levels of CXCL12 and SCF, thus mediating HSC maintenance and retention[33,34]. Of note, CXCL12-expressing cells, or CXCL12-abundant reticular (CAR) cells, are the main regulators of HSCs, although the exact composition of CAR cells is still unknown[34]. Deletion of CAR cells leads to a significant decrease in HSC number in the bone marrow compartment[34].

Sympathetic nerves are also involved in the trafficking of HSCs during homeostasis. Nestin$^+$ cells, many of which are also CAR cells, contact with sympathetic nerves directly in the bone marrow[35]. By β3-adrenergic receptor signaling pathway, Nestin$^+$ cells downregulate HSC

maintenance genes including CXCL12 and Angpt1. Another cellular component of neuronal system, Nonmyelinating Schwann cells, also co-localize with HSCs and activate transforming growth factor-β (TGF-β)-SMAD signaling pathway, keeping HSC in a quiescence state[35].

1.6 BM suppression of hematopoietic stem cells

Bone marrow cells are very sensitive to stress including chemotherapeutic agents and ionizing radiation. This limits the dose of therapies in hematologic malignancies and disorders. A couple of hematopoietic growth factors, including erythropoietin (EPO), granulocyte-colony stimulating factor (GCSF) and granulocyte-macrophage stimulating factor (GMCSF), have been used to protect HSCs during the therapy[36].

The risk of radiation exposure has been increased in the modern society. High radioactive sources such as cobalt-60 and cesium-137 previous used in radiotherapy machines can cause local skin injuries or acute radiation syndrome to the operators. Radiation can target rapidly dividing cells including bone marrow cells. The effect of radiation is dependent on the dose. Low dose radiation does not cause cell death, but increases the chance of malignant mutation[36]. For radiation dose above 10Gy, the mortality significantly increases[36]. Long-term defects of radiation on HSCs have also been reported previously, including HSC senescence, and deficit in bone marrow transplantation[37,38].

Our lab found that systemic administration of a neurite outgrowth factor, pleiotrophin (PTN), promotes a significant expansion of bone marrow stem and progenitor cells in vivo[39]. In addition, injection of PTN significantly increases the survival of irradiated mice, potentially by regulating proliferation of hematopoietic progenitors after irradiation[40]. Of note, PTN treatment has significantly better therapeutic effect compared to mice treated with saline or GCSF[39]. In another study, we found that epidermal growth factor (EGF) signaling to be upregulated in the bone

marrow serum after radiation. Treatment of EGF significantly promotes HSC regeneration in vivo, as can be determined by the increasing number of whole bone marrow cells, KSL cells, colony-forming cells and CFU-S12[41]. Finally, our lab found that inhibition of aldehyde dehydrogenase (ALDH) with diethylaminobenzaldehyde (DEAB) significantly increases the number of HSCs in culture compared to control cells[42].

Research from other labs also suggests the involvement of Akt-mTOR and Notch signaling pathways in the HSC regeneration[40]. Other factors including angiocrine factors fibroblast growth factor 2 (FGF2), insulin-like growth factor binding protein 2 (IGFBP2), Angiopoietin-1 (ANGPT1), bone morphogenetic protein 4 (BMP4) and desert hedgehog (DHH), are also involved in the regeneration of HSCs[43].

Chemotherapy is another main source of hematopoietic injury. Current chemotherapy method includes antimetabolites, DNA-damaging drugs and tyrosine kinase inhibitors[44,45]. 5-fluorouracil (5FU) is often used in hematopoietic regeneration studies because of its limited toxicity. 5FU has been widely used to enrich hematopoietic stem cells by induction of death to the dividing cells.

1.7 Grb10 family of adaptor proteins

The Grb (growth factor receptor-bound) family of proteins are a group of cellular adaptor proteins that have no intrinsic enzymatic activity. There are three members in the Grb family: Grb7, Grb10 and Grb14[46]. Originally, Grb family members were identified by CORT (cloning of receptor targets) screens with autophosphorylated C-terminus of the EGFR as a probe to screen for interacting proteins[47].

Grb family member share a common GM (Grbs and Mig) region in the center, which is 60% identical between Grb7, 10 and 14[48]. The GM region can be further divided into RA (Ras-association)-like and PH (pleckstrin homology) domains. An SH2 (Src homology 2) domain is

located at the C-terminus of the protein and is the primary binding site to phospho-tyrosines of growth factor receptors and intracellular signaling proteins. The signature domain for the Grb family proteins is called BPS (between the PH and SH2 domains)[49].

Previous data indicates that, murine Grb10 mRNA is highly expressed in insulin target tissues, including skeletal muscle, adipose tissue, heart and kidney[50]. In addition, Grb10 is highly expressed in fetal liver but not adult liver tissues[51]. Grb14 has a similar expression pattern as Grb10[52]. The expression of Grb7 is unique that Grb7 mRNA is not detected in murine skeletal muscle, but is highest in the liver and kidney[53].

Expression of Grb family member proteins in humans generally correlates with the murine expression profile. Besides the high expression of hGrb10 in skeletal muscle, hGrb10 also has high expression in pancreas[54]. hGrb10 also has intermediate expression in cardiac muscle and brain, while the expression in the other tissues are trivial. As for hGrb14, the expression is high in liver and heart, and relatively low in a variety of other tissues including human skeletal muscle, pancreas, kidney and gonads[55]. Overall, hGrb10 and hGrb14 exhibit similar expression patterns while the expression of hGrb7 is unique, with limited expression mainly in pancreas, prostate, liver and small intestine[54].

Grb family members have the potential to bind to numerous receptor tyrosine kinases through their SH2 domain[46]. For example, it has been well characterized that Grb10 and Grb14 bind to insulin receptor (IR) and IGFR (insulin-like growth factor receptor), although the binding to the latter is much weaker. Biochemical assays, including yeast-two hybrid screen or pull down assays, have shown that Grb family members interact with c-kit/SCFR (stem cell factor receptor), EphB1, ErbB2/3/4, FGFR (fibroblast growth factor receptor) and PDGFβR (platelet-derived growth factor β-receptor), Ret and Tek (tunica endothelial kinase)/Tie2[46,47].

It is of note that Grb10 has a stronger binding capability to IR compared to IGFR. However, the mechanism to explain the differential binding capability of the SH2 domain to the IR and IGFR has not been clearly illuminated. Binding of Grb10 and Grb14 to IR has been shown to inhibit the downstream activation of PI3K (phosphoinositide 3-kinase) and protein kinase B/Akt, in some situations Erk/MAPK signaling as well[46]. On the contrary, research from another lab suggests that Grb10, specifically, may have positive regulatory role in the regulation of insulin and other growth factor signaling pathway[47]. With an overexpression model, they found that Grb10 promotes cell proliferation under the setting of insulin, IGF-1 or PDGF-BB treatment[56]. One possible explanation for the inconsistency in the data regarding to the role of Grb10 is that these studies are utilizing an overexpressing model with various cell lines, some of which have no expression of Grb10 under physiological conditions. The most definitive data comes from the knockout studies in mice. In one mouse model where Grb10 was disrupted by a gene-trap insertion, Grb10 deficient mice show both embryo and placenta overgrowth compared to littermate control[57]. Grb14 deficient mice show increased tolerance of glucose by elevating the incorporation of glucose into glycogen. This phenotype is mediated by the increased activation of insulin signaling pathway[58].

Several potential mechanisms have been proposed to explain the function of Grb10. Grb10 activation was shown to decrease the phosphorylation of receptors such as IR, although data from different research groups have been controversial[59,60]. In addition, Grb10 was shown to interact with Nedd4, a critical protein involved in protein degradation[61]. Grb10 overexpression leads to the increased ubiquitination of the IGFR and eventually the accelerated degradation of the receptor[62]. Moreover, other data suggest that Grb10 is involved in the regulation of apoptosis. Grb10 binds to Raf-1 and MEK1 through its SH2 domain[63]. The disruption of this binding in

cells induces apoptosis, although the detailed mechanism has not been clearly identified. Finally, research shows that Grb7 regulates cell migration induced by growth factor signaling[64]. However, there were few studies on the effect of Grb10 on cell migration.

1.8 Imprinted gene network

The phenomenon of gene imprinting has been observed for decades. With the two alleles of gene inherited (one from mother and one from father), the imprinted genes are only expressed from one allele. Current evidence shows that the parental legacy is controlled on the epigenetic level—by histone modifications including DNA methylation[65].

Among all the imprinted genes, a subset of them, named imprinted gene network (IGN), have been shown to have down-regulation of mRNA expression with age in multiple organs[68]. These genes include Igf2, H19, Plagl1, Mest, Peg3, Dlk1, Gtl2, Grb10, Ndn, Cdkn1c and SLC38a4. This decline in expression correlates well with the decrease in growth rate, indicating a potential cell proliferation control mechanism by gene imprinting[68]. Another research shows that, within the IGN, Grb10, Gtl2, H19, Ndn and Peg3 are predominately expressed in murine LT-HSCs, while the expression of Gatm, Plagl1 and Sgce are significantly higher in the murine LT-HSCs compared to mature hematopoietic cells[69]. Interestingly, Grb10 shows increased expression in the LT-HSCs after 5-FU treatment, suggesting a potential regulatory role of Grb10 in the HSC regeneration[68]. Data from human bone marrow cells also confirmed that most of the IGN genes have elevated expression in the stem cell portion[68]. Of note, expression data from mouse muscle and skin tissues show that IGN gene expression is enriched in the stem cells within these tissues[68]. These data lead to a model that the expression level of IGN genes is an indicator of tissue development. In the embryogenesis when the growth potential is highest, IGN genes are highly expressed and regulate the development process. During the maturation, the expression of

IGN is decreased gradually in the non-stem somatic cells. However, in the somatic stem cells where the growth potential is partially retained, the expression of IGN genes are still high, although not comparable to the expression level in embryo[68].

Recently researches in hematopoietic stem cells have started to show evidence of the model that IGN regulates development. Deletion of the maternal but not paternal differentially methylated region upstream of H19 (H19-DMR), changes the adult hematopoietic stem cells from a quiescence state to active proliferation state, thus compromises hematopoietic stem cell function[70]. This phenotype is potentially mediated by the elevated Igf2-Igfr1 signaling pathway. In another study, the imprinted Dlk1-Gtl2 locus, that produces multiple non-coding RNAs (ncRNAs) maternally, was shown to have a critical role in preserving LT-HSCs[71]. Mechanistically, the miRNA expressed from the Dlk1-Gtl2 locus functions as negative regulators of PI3K-mTOR signaling pathway, and induces inhibition of mitochondrial biogenesis. More research on other genes in IGN will be needed in order to link the IGN to the "stemness" of the hematopoietic stem cells.

1.9 RhoGTPase family member of proteins and its relation with hematopoiesis

Rho family of GTPase is a group of proteins that regulates cytoskeleton, migration and adhesion. The activity of individual Rho proteins can be regulated by two kinds of signaling molecules, guanine exchange factors (GEFs) and GTPase-activating proteins (GAPs)[72]. Most of the Rho GTPase is expressed ubiquitously. However, Rac subfamily of RhoGTPase (Rac1, Rac2 and Rac3) have been shown to be particularly important for hematopoietic cells. While another identified hematopoietic-specific Rho GTPase, RhoH, have been shown to modulate Rac signaling[73]. Crosstalks from different subgroups of Rho GTPases have also been discovered. Cdc42, Rac and RhoA can influence each other's function, either by stimulation or inhibition.

Rac1 and Rac2 in hematopoiesis

With a knockout mice model, Rac1-deficient HSCs have demonstrated deficit in the response to extracellular signaling such as SCF[74], while the Rac2-deficiency leads to the increased apoptosis in HSCs in response to SCF[74]. Studies also show that, mouse mutants of Rac1 and/or Rac2 reveal the involvement of Rac family proteins in the regulation of HSC adhesion, migration, degranulation and cell shape change[75]. Rac1 and Rac2 have also been shown to be linked to cell proliferation and survival. Altogether, Rac GTPases are important molecular switches for the localization of the stem cells in the bone marrow microenvironment. A novel molecule inhibitor, NSC23766, has been developed to promote the mobilization of the HSC, which has great clinical value[74].

Rac3 and its role in the hematopoiesis

Rac3 was identified from a chronic leukemia cell line and is the third member of the Rac subfamily. Rac3-/- mice have not shown major abnormalities, although one group has found a really subtle neurological phenotype[76]. Interestingly, although no functional relationship has been suggested in the hematopoiesis, the expression of Rac3 is significantly decreased in the differentiated cell population, suggesting a potential relationship between Rac3 and "stemness"[77]. One possible explanation is that the function of Rac3 is inhibited by the Rac2 expression[78]. However, further research will need to be conducted in order to conclude on the real function of Rac3 on stem cells.

Cdc42 in hematopoiesis

Previous research indicates a functional role of Cdc42 in the regulation of gradient sensing and filopodia[79]. In lymphocytes, a dominant negative form of Cdc42, is closely related to the disruption in cell polarization and reduced response to SDF1 (CXCL12), which is one of the

most potent chemokine for lymphocytes[80]. In two mouse models, inhibition of Cdc42, by genetic deletion of the Cdc42 GEF, decreases the capability of cell migration by influencing G-coupled receptor signaling and PAK activation[72]. On the other hand, overactivation of Cdc42 activity, by knockout of Cdc42 GAP protein, leads to a significant increase in the cell death profile in the HSC population[72]. As for the mature hematopoietic cells, Cdc42 deficient neutrophils have enhanced capability to mobilize, but the migration is decreased due to a deficient in the podosome-like structure[81]. In accordance with this, $Cdc42^{-/-}$ mice have increased number of HSC in the blood, indicating a deficiency in the homing of HSCs to the bone marrow niche[82]. In addition, $Cdc42^{-/-}$ mice show a myeloproliferative disorder as shown by the abnormal increase in neutrophils and other myeloid cells as well as by the increased number of colony-forming cells (CFCs) with $Cdc42^{-/-}$ bone marrow cells[72].

RhoA in hematopoiesis

Compared to the extensive study on Rac and Cdc42, the role of RhoA on hematopoiesis has been less studied. RhoA activation has fundamental effect on cell cycle, by regulating the expression of cyclin D-Cdk4 in the cell cycle and promotes cells to go into DNA replication phase[83]. In an overexpressing model using a dominant negative form of RhoA GTPase, a group discovered that RhoA inhibition promotes HSC engraftment and reconstitution in the bone marrow transplantation assay[84]. RhoA was also closely involved in the regulation of hematopoietic progenitor migration in vitro.

1.10 mTOR signaling and its relation with hematopoiesis

mTOR signaling pathway has been involved in a variety of cellular processes such as growth and proliferation, and the disruption of normal mTOR signaling leads to human disease including cancer, obesity, diabetes and neurodegeneration[85]. There are two mTOR complex in the humans,

mTOR complex 1 (mTORC1) and 2 (mTORC2). Both of the mTOR complexes are comprised of several proteins: mTORC1 has six and mTORC2 has seven components. Among the different protein components, DEP domain containing mTOR-interacting protein (DEPTOR) was shared by both complex 1 and complex 2[86]. On the contrary, a protein called regulatory-associated protein of mammalian target of rapamycin (raptor) is specific to mTORC1, while another protein, named rapamycin-insentivie companion of mTOR (rictor) is unique to mTORC2[87,88].

mTORC1

mTORC1 is capable of integrating five different signals, including growth factors, stress, energy status, oxygen, and amino acids, and controls different cellular processes[85]. Directly upstream of mTORC1 is the protein heterodimer tuberous sclerosis 1 (TSC1) and TSC2. Previous report indicates that TSC1/TSC2 directly regulates signaling from insulin and insulin-like growth factor 1 (IGF1)[85]. In another report, Wnt signaling was shown to be activators of mTORC1 through TSC1/TSC2 complex[89]. Finally, tumor necrosis factor-α (TNF α) can also activate mTOR signaling pathway by regulating the function of the same complex[90]. Interestingly, stresses are also powerful inducers of mTORC1 signaling. For example, hypoxia or low energy stress increases the activity of TSC2, thus inhibits mTORC1 signaling[91]. DNA damage is the other main resource for mTORC1 activation, and it usually involves the p53-signaling pathway[85].

On the downstream, mTORC1 phosphorylates 4E (elF4E)-binding protein 1 (4E-BP1) and S6 kinase 1 (S6K1) and initiate protein synthesis[92]. In addition to 4E-BP1 and S6K1, mTORC1 also activates tripartite motif-containing protein-24 (TIF-1A), and enhanced the binding of TIF-1A to RNA polymerase I (Pol I)[93]. Another main function of mTORC1 is the regulation of lipid synthesis[94]. mTORC1 regulates sterol regulatory element-binding protein ½ (SREBP1/2), resulting in an active form of SREBPs, which then initiate the transcription of lipogenic

genes[95,96]). Finally, mTORC1 has been reported to increase the activity of hypoxia inducible factor 1α (HIF1α), and thus regulate the cellular metabolism and ATP production[95,97].

mTORC2

The relationship between mTORC2 and rapamycin has been controversial. At first it was described to be rapamycin insensitive, but recent research has thrown light upon the new function of rapamycin, that prolonged treatment of rapamycin significantly reduces the signaling through mTORC2[87,98,99]. Signals through mTORC2 have been shown to be selective, because only part of the downstream molecules, including forkhead box O1/3a (FoxO1/3a), but not GSK3-β[100,101]. Another key downstream regulator is PKC-α, which is involved in the cell shape regulation[87,102].

mTOR and hematopoiesis

mTOR signaling has long been closely involved in the regulation of HSC function. The deletion of PTEN, a negative regulator for mTORC1, leads to the depletion of HSCs by the overexpression of p16 and p53 in HSCs, and the overexpression of p19 and p53 in other hematopoietic cells[103]. In another study, tissue-specific deletion of Raptor shows a nonlethal phenotype and mice lack Raptor expression have pancytopenia, splenomegaly and increased number of monocytes[104]. Raptor is essential for the regeneration of HSCs, which is the first signaling molecule in the mTOR signaling pathway. Induced deletion of TSC, the negative regulator of mTOR, leads to rapid cycling of HSCs and eventually depletion, through the generation of reactive oxygen species (ROS)[105]. Co-treatment of canonical Wnt-β-catenin signaling activator, together with rapamycin to inhibit mTOR signaling pathway, maintain both human and mouse long-term HSCs in a cytokine-free condition[106]. mTOR was also shown to be involved in the aging of HSCs. One study reveals that mTOR signaling activity is increased in

the old mice compared to the young mice, and systemic treatment of rapamycin to old mice rejuvenate the aging HSCs[107]. More research will need to be conducted to decipher the function of mTOR signaling pathway on HSCs.

Chapter 2 Deletion of the imprinted gene, Grb10, promotes hematopoietic stem cell self-renewal and regeneration

2.1 Grb10 expression is enriched in regenerating BM HSCs.

2.1.1 Methods

Mice. All animal procedures were performed in accordance with Duke and UCLA IACUC-approved animal use protocols. C57BL/6 mice and B6.SJL mice between 8-12 week old were obtained from Jackson Laboratory (Bar Harbor, ME) and housed at Duke University Cancer Center Isolation Facility and the University of California – Los Angeles Radiation Oncology Animal Care Facility.

Microarray analysis. C57BL6 mice were irradiated at 550cGy TBI with a Shepherd Mark I 68A Cesium-137 (Cs^{137}) gamma-irradiator. At day+ 14, bone marrow c-kit+sca-1+lineage- (KSL) cells were isolated by flow cytometric cell sorting as previously described[39]. Genomic RNAs from irradiated KSL cells and non-irradiated control KSL cells were isolated with Qiagen RNeasy Micro Kit (Qiagen, MD). Total RNA were assessed for quality with Agilent 2100 Bioanalyzer G2939A (Agilent Technologies, Santa Clara, CA)) and Nanodrop 8000 spectrophotometer (Thermo Scientific/Nanodrop, Wilmington, DE). Hybridization targets were prepared from total RNA with the NuGen WT-Ovation Pico RNA Amplification kit (NuGen Technologies, San Carlos, CA) followed by the NuGen FL-Ovation Biotin Module V2 (NuGen Technologies, San Carlos, CA). Amplified, labeled cDNA was then hybridized to GeneChip® Mouse Genome 430A 2.0 arrays in Affymetrix GeneChip® hybridization oven 645, washed in

Affymetrix GeneChip® Fluidics Station 450 and scanned with Affymetrix GeneChip® Scanner 7G according to standard Affymetrix GeneChip® Hybridization, Wash, and Stain protocols. (Affymetrix, Santa Clara,CA).Amplified RNA samples then were loaded onto GeneChip Mouse Genome 430A 2.0 arrays (Affymetrix). We analyzed the microarray data with Partek Genomics Suite and generated lists of differentially expressed genes triggered by irradiation, as previously described[108]. Quantile normalization method was used to normalize the gene expression and raw data was log2 transformed. Differentially expressed genes were identified using the Partek software. ANOVA (Analysis of variance) was used to calculate the p value. Genes showing altered expression with $p < 0.05$ and more than 2 fold changes were considered differentially expressed. The pathway and network analysis was performed using Ingenuity (IPA). IPA computes a score for each network according to the fit of the set of supplied focus genes. These scores indicate the likelihood of focus genes to belong to a network versus those obtained by chance. A score > 2 indicates a <= 99% confidence that a focus gene network was not generated by chance alone. The canonical pathways generated by IPA are the most significant for the uploaded data set. Fischer's exact test with FDR option was used to calculate the significance of the canonical pathway.

Quantitative real-time PCR. RNA was isolated using the Qiagen RNeasy micro kit. RNA was reverse transcribed into cDNA using iScript cDNA synthesis kit. Using Taqman Gene Expression assays, we performed real time PCR analysis for Grb10, Socs2, Adrb2, Ccl3 and Ccl4.

Flow cytometry. BM cells were flushed out from the hinder bones (tibias and femurs) by a 25-gauge needle with 1X DPBS plus 10% FBS, 1% penicillin-streptomycin. Collected BM cells were stained with APC-Cy7-conjugated anti-ckit (BD Biosciences), PE-conjugated anti-sca-1

(BD Biosciences), V450-conjugated anti-lineage (BD Biosciences). Flow cytometry analysis was performed on a FACS CANTO II (BD Biosciences).

Human cord blood collection. Human umbilical cord blood (CB) were obtained from the Carolinas Cord Blood Bank at Duke University Medical Center. The protocol was approved by the Institutional Review Board of Duke University. Human cord blood cells were separated by slowly adding cord blood onto the top of a lymphoprep (Stemcell Technologies Inc, Vancouver, BC), and centrifuging for 30min. Red blood cells were lysed twice with ACK lysis buffer (Lonza). Lin^+ mature hematopoietic cells were depleted by StemStep human hematopoietic progenitor cell enrichment kit (Stemcell Technologies). To isolated human $Lin^-CD34^+CD38^-$ cells, lineage-depleted Lin^- human cells were incubated with PE-conjugated anti-CD34 (BD Biosciences), FITC-conjugated anti-CD38 (BD Biosciences) for 30 min and sorted with FACS Aria II cell sorter (BD Biosciences).

Statistical analyses. Data were expressed as the means ± s.e.m. Differences between two groups were analyzed with the student's t test (two-tailed with unequal variance), unless otherwise indicated in the Figure Legends. Competitive repopulating assays were compared with a two-tailed Mann-Whitney test. GraphPad Prism 6.0 was used for all statistical analyses. For all animal studies, we used a power test to determine the sample size needed for a 2-fold difference in mean with 0.8 power using a two-tailed student's t-test. Animals in our studies were sex and age-matched and wild-type littermates were used as controls.

2.1.2 Results

In order to identify novel candidate genes that regulate HSC regeneration, we irradiated B6 mice at 550cGy and monitored the recovery of bone marrow c-kit^+sca-$1^+$$lineage^-$ (KSL) cells, which are enriched for hematopoietic stem/progenitors. After bone marrow irradiation, KSL cells were

quickly depleted from bone marrow, and gradually show signs of the initial recovery between day+10 and day+14 after irradiation (**Figure 1**).

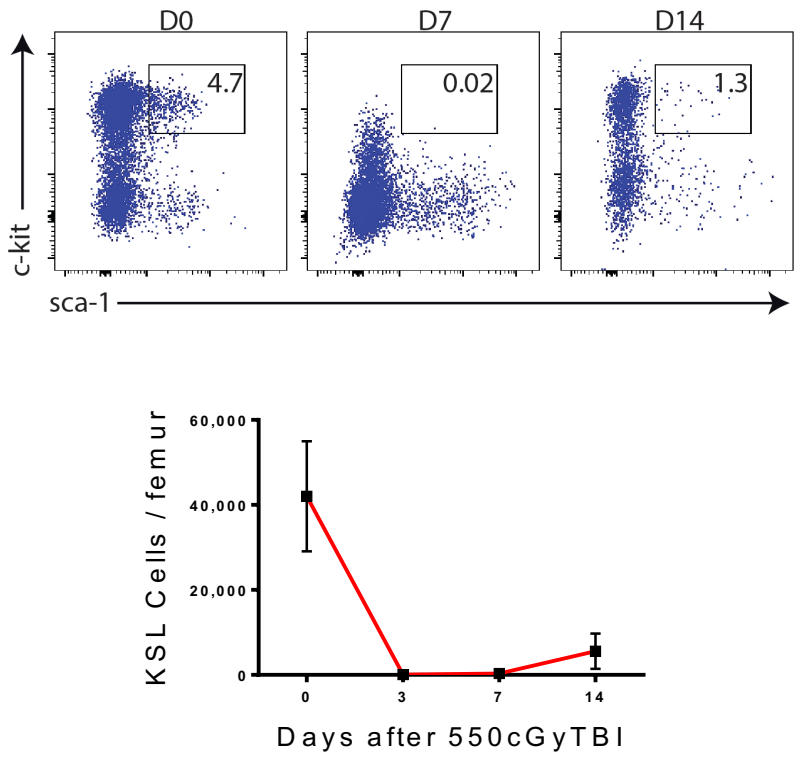

Figure 1 The time course of hematopoietic stem cell regeneration.

Upper, 10-12wks old C57Bl6 mice received 550cGy TBI and bone marrow c-kit+sca-1+lineage- (KSL) cells were evaluated by flow cytometric analysis at indicated time points following irradiation. Percentage of KSL cells was shown in the gate (n = 8 mice/group). Lower, KSL cells per femur over time following 550cGy TBI (n = 8 mice /time point).

To capture the regenerative phase of hematopoietic stem cells after irradiation, we utilized fluorescence-activated cell sorting and isolated murine BM c-kit^{+}sca-1^{+}lineage^{-} (KSL) cells from adult C57Bl6 mice at day +14 following 550cGy total body irradiation (TBI), as this is the

earliest time point at which BM KSL cells are readily detectable following myeloablative irradiation. We then performed high-throughput microarray analysis and compared the gene expression profile between irradiated KSL cells versus non-irradiated control (**Figure 2**). A list of genes is up- and down-regulated by the irradiation damage, many of which have no already known role in hematopoiesis.

Among all the genes that show differential expression in response to irradiation, we are particularly interested in growth factor receptor-bound protein (Grb10), that has no already known role in hematopoiesis.

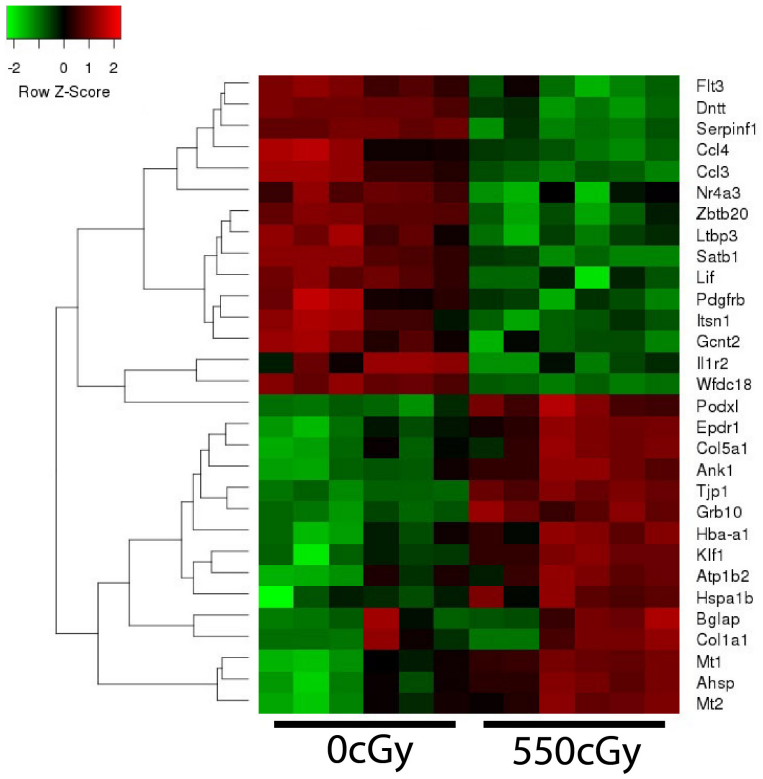

Figure 2 Heatmap of KSL cell gene expression after irradiation

10-12wks old C57Bl6 mice were irradiated at 550cGy TBI and KSL cells were isolated at day+14 following irradiation. Microarray analyses were performed with irradiated KSL cells compared to non-irradiated control. Heat map shows the top genes that were up- or down-

regulated by irradiation (n = 6 mice/sample, n = 6 samples /group. Red, increased expression; green, decreased expression).

With RT-PCR, we confirmed the expression of five genes that have highest fold-change induced by irradiation (**Figure 3**). Grb10 was 5.5-fold higher in irradiated BM HSCs compared to non-irradiated HSCs. Suppressor of cytokine signaling 2 (Socs2), a member of the STAT-induced STAT inhibitor (SSI) was shown to be significantly up-regulated by irradiation in KSL cells. Within the genes that show downregulation caused by irradiation, the beta-2 adrenergic receptor (β_2 adrenoreceptor) was downregulated by 5-fold in KSL cells in response to irradiation. Epinephrine binds to adrb2, and leads to physiologic responses. The downregulation of adrb2 in KSL cells after irradiation indicates the potential involvement of neuronal control in hematopoietic stem cell regeneration. Interestingly, two cytokines, chemokine (C-C motif) ligand 3 (CCL3) and CCL4, were also shown to be downregulated by irradiation in KSL cells. CCL3 and CCL4 attract and bind to each other, together they serve as a chemoattractant for macrophage, monocytes and neutrophils. To determine the specificity of the expression of these genes, we performed RT-PCR with c-kit$^+$sca-1$^-$lineage$^-$ hematopoietic progenitor-enriched cells (**Figure 4**). Surprisingly, Grb10 shows no differential expression in the progenitor cells post irradiation. These data indicate that Grb10 has unique regulatory role in the irradiation response of bone marrow KSL cells.

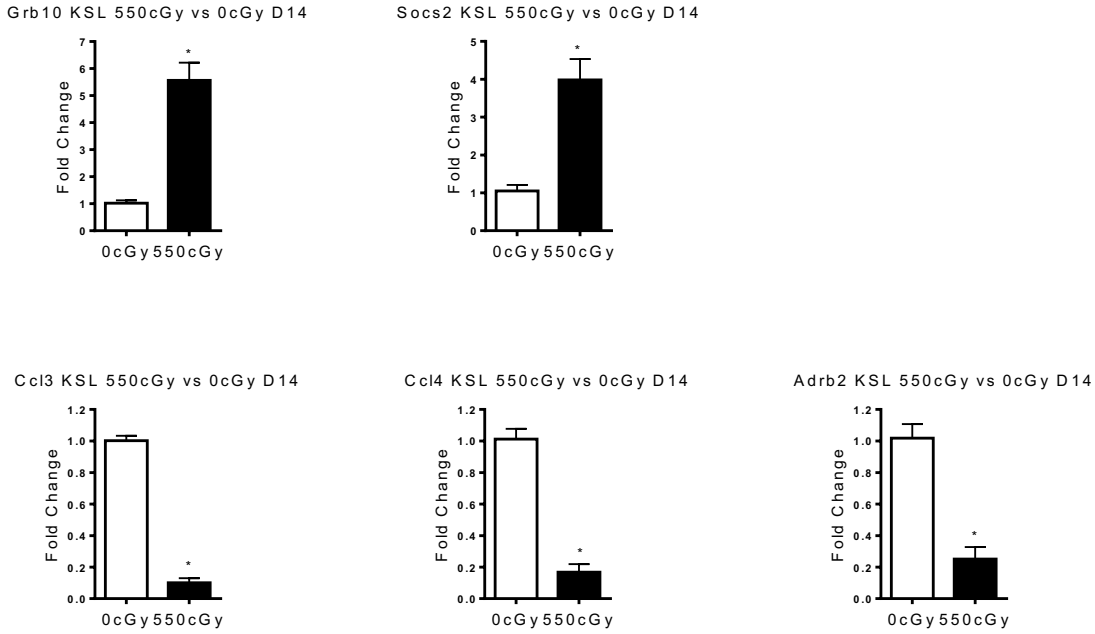

Figure 3 RT-PCR of 5 selected genes at day+14 after 550cGy irradiation

Mean expression of Grb10 in BM KSL cells before and at day+14 following 550cGy TBI, as determined by quantitative reverse-transcriptase PCR (qRT-PCR). Samples were normalized to 0cGy KSL cells, respectively (n = 6/group, t-test).

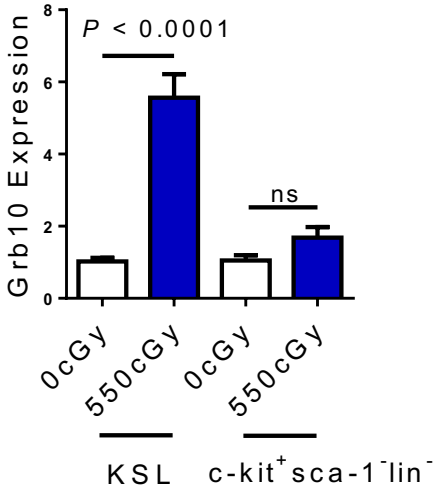

Figure 4 Expression of Grb10 at KSL and c-kit$^+$sca-1$^-$lin$^-$ cells after irradiation

Mean expression of Grb10 in BM KSL cells and c-kit$^+$ sca-1$^-$ lineage$^-$ cells before and at day+14 following 550cGy TBI, as determined by quantitative reverse-transcriptase PCR (qRT-PCR). Samples were normalized to 0cGy KSL cells and 0cGy c-kit$^+$ sca-1$^-$lineage$^-$ cells, respectively (n = 6/group, t-test).

Grb10 was shown to be a negative regulator of signaling through receptor tyrosine kinase. Of all the receptors Grb10 binds to, many of them, such as Tie2, c-kit and FGFR, have critical roles in the maintenance of "stemness" at steady state. These data indicate a potential involvement of Grb10 in the HSC maintenance. We isolated different portions of bone marrow cells, and used RT-PCR to determine the expression of Grb10 (**Figure 5**). Compared to the expression level of Grb10 in whole bone marrow cells, Grb10 was highly expressed in the Lin$^-$ cells and KSL cells, and have more than 30-fold higher expression in CD34$^-$KSL cells. These data indicate that the expression of Grb10 is correlated with the "stemness" of the HSCs and Grb10 is a potential regulator of HSC maintenance. To further confirm the role of Grb10, we isolated human cord blood stem cells and performed RT-PCR (**Figure 6**). Compared to total mononuclear cells, Grb10 expression was elevated in the Lin$^-$CD34$^+$ cells, which is enriched for the human hematopoietic stem cells. However, further enrichment of human hematopoietic stem cells by staining Lin$^-$CD34$^+$CD38$^-$ did not increase the expression level of Grb10. In clinical applications, CD34$^+$ enrichment has been shown to have faster donor engraftment and less clinical complications, thus the overexpression of Grb10 in the CD34$^+$ portion of cord blood cells have important clinical value[109].

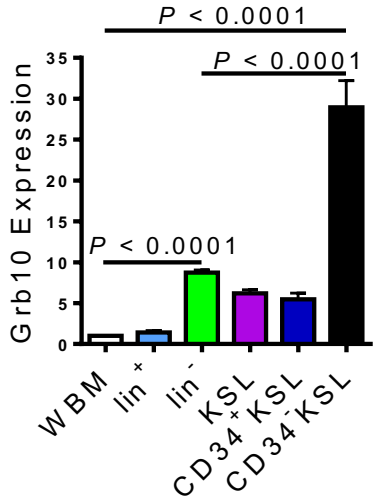

Figure 5 Expression of Grb10 in murine BM

Mean expression of Grb10 in different populations of BM cells by qRT-PCR. WBM, whole bone marrow cells (n = 6-10 mice/group).

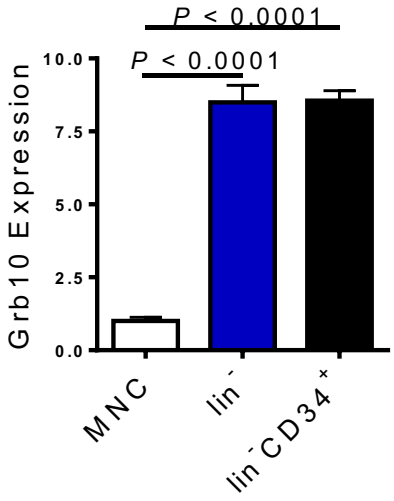

Figure 6 Expression of Grb10 in human cord blood

qRT-PCR shows the mean expression of Grb10 in different fractions of human cord blood. MNC, mononuclear cells (n = 8 / group, t-test).

2.2 Grb10 ablation promotes HSC engraftment capability

2.2.1 Methods

Mice. All animal procedures were performed in accordance with Duke and UCLA IACUC-approved animal use protocols. *Grb10*$^{m/+}$ mice were a kind gift from Dr. Andrew Ward's group (University of Bath, UK). *Grb10*$^{m/+}$ mice were maintained in a mixed background of C57BL/6: CBA until backcrossed into a C57BL/6 background. The genetic background of backcrossed mice was confirmed using the genome scanning service from Jackson Laboratory (Bar Harbor, ME). C57BL/6 mice and B6.SJL mice between 8-12-week-old were obtained from Jackson Laboratory (Bar Harbor, ME).

Mouse competitive repopulating unit assays. Mouse whole bone marrow cells were isolated from 10-12-week-old Grb10$^{m/+}$ and Grb10$^{+/+}$ mice expressing CD45.2^{+} allele. Recipient 10-week old CD45.1^{+} B6.SJL mice were irradiated with 950cGy TBI using a Cs 137 irradiator 24h before bone marrow transplantation. 2 x 10^5 whole bone marrow cells from either *Grb10*$^{m/+}$ or *Grb10*$^{+/+}$ mice were injected via tail vein into recipient mice along with a competing dose of 2 x 10^5 non-irradiated host BM cells. Multilineage hematopoietic cell engraftment was monitored by flow cytometry analysis of the peripheral blood at 4, 8, 12, 16 and 20 weeks posttransplant, as previous described[23,40]. To perform the secondary competitive transplant assay, B6.SJL mice were irradiated with 950cGy TBI and used as secondary recipients. By volume, 75% of bone marrow cells of the primary recipients were injected via tail vein into the secondary recipients together with 2 x 10^5 host competitor bone marrow cells from the B6.SJL mice. PB samples of the secondary recipients were monitored by flow cytometry at 4, 8, 12 and 16 weeks posttransplant.

Quantitative real time PCR. RNA was isolated using the Qiagen RNeasy micro kit. RNA was reverse transcribed into cDNA using iScript cDNA synthesis kit. Using Taqman Gene Expression assays, we performed real time PCR analysis for p16, p21 and p27.

Flow cytometry. BM cells were flushed out from the hinder bones (tibias and femurs) by a 25-gauge needle with 1X DPBS plus 10% FBS, 1% penicillin-streptomycin. Collected BM cells were stained with APC-Cy7-conjugated anti-c-kit (BD Biosciences), PE-conjugated anti-sca-1 (BD Biosciences), V450-conjugated anti-lineage (BD Biosciences), FITC-conjugated anti-CD48 (Biolegend), and Alexa Fluor 647-conjugated anti-CD150 (Biolegend).

Histology. Hematoxylin and eosin (H&E) staining of femurs from mice was performed as previously described[40]. Femurs were fixed overnight in 10% formalin, followed by decalcification and paraffin embedding. Images were obtained using an Axiovert 200 microscope (Carl Zeiss, Thornwood, NY).

Statistical analyses. Data were expressed as the means ± s.e.m. Differences between two groups were analyzed with the student's t test (two-tailed with unequal variance), unless otherwise indicated in the Figure Legends. Competitive repopulating assays were compared with a two-tailed Mann-Whitney test. GraphPad Prism 6.0 was used for all statistical analyses. For all animal studies, we used a power test to determine the sample size needed for a 2-fold difference in mean with 0.8 power using a two-tailed student's t-test. Animals in our studies were sex and age-matched and wild-type littermates were used as controls.

2.2.2 Results

Grb10 was one of the genes that are genetically imprinted. Of the two alleles of Grb10 in human, only one of them is expressed. Previous data suggest that Grb10 is mainly maternally imprinted in most of the mouse tissues except brain. In order to test whether Grb10 regulates

hematopoiesis, we obtained Grb10 gene trap mutant mice (Grb10Δ2-4 mice)[57] and extensively backcrossed this strain into the C57Bl6 strain. Paternal inheritance of Grb10Δ2-4 ($Grb10^{+/p}$ mice) caused no significant alteration in Grb10 expression in BM cells, but caused significantly decreased expression in the brain (**Figure 7**). In contrast, maternal inheritance of Grb10Δ2-4 ($Grb10^{m/+}$ mice) caused significantly decreased expression of Grb10 in BM $lineage^-$ cells, with no effect on expression in the brain.

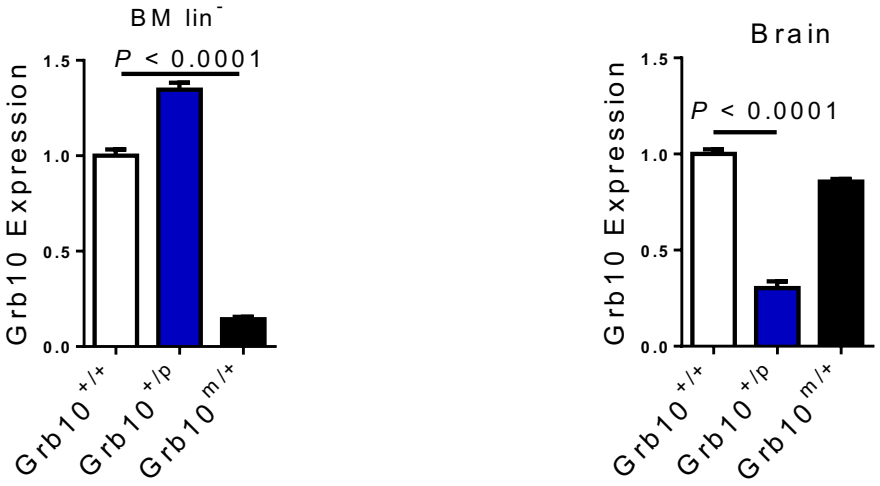

Figure 7 Effect of imprinting in Grb10 maternal and paternal deletion mice

Expression of Grb10 in left, $lineage^-$ cells and right, brain of C57Bl6 mice. $Grb10^{+/P}$, mice with Grb10 paternal deletion; $Grb10^{m/+}$, mice with Grb10 maternal deletion (n = 3 mice / group). (b) Complete blood counts of peripheral blood comparing $Grb10^{m/+}$ mice with $Grb10^{+/+}$ mice (n = 8 – 10 mice/group, t-tests).

Because of the structure similarity in the Grb10 family member proteins, we also examined the expression level of other members in the Grb10 family, to evaluate the potential compensation of other Grb proteins in the case of Grb10 ablation. The expression of Grb10 was significantly

decreased in most of the tissues we examined, including BM, Lin$^-$, spleen and peripheral blood (**Figure 8**). However, the expression of Grb7 and Grb14, the other two well-known members of the Grb family of adaptor protein, have very limited expression in the hematopoietic system and the expression of both Grb17 and Grb14 were not influenced by Grb10 ablation. Based on all these data, we therefore focused on the effect of maternal inheritance of Grb10Δ2-4 on the hematopoietic system.

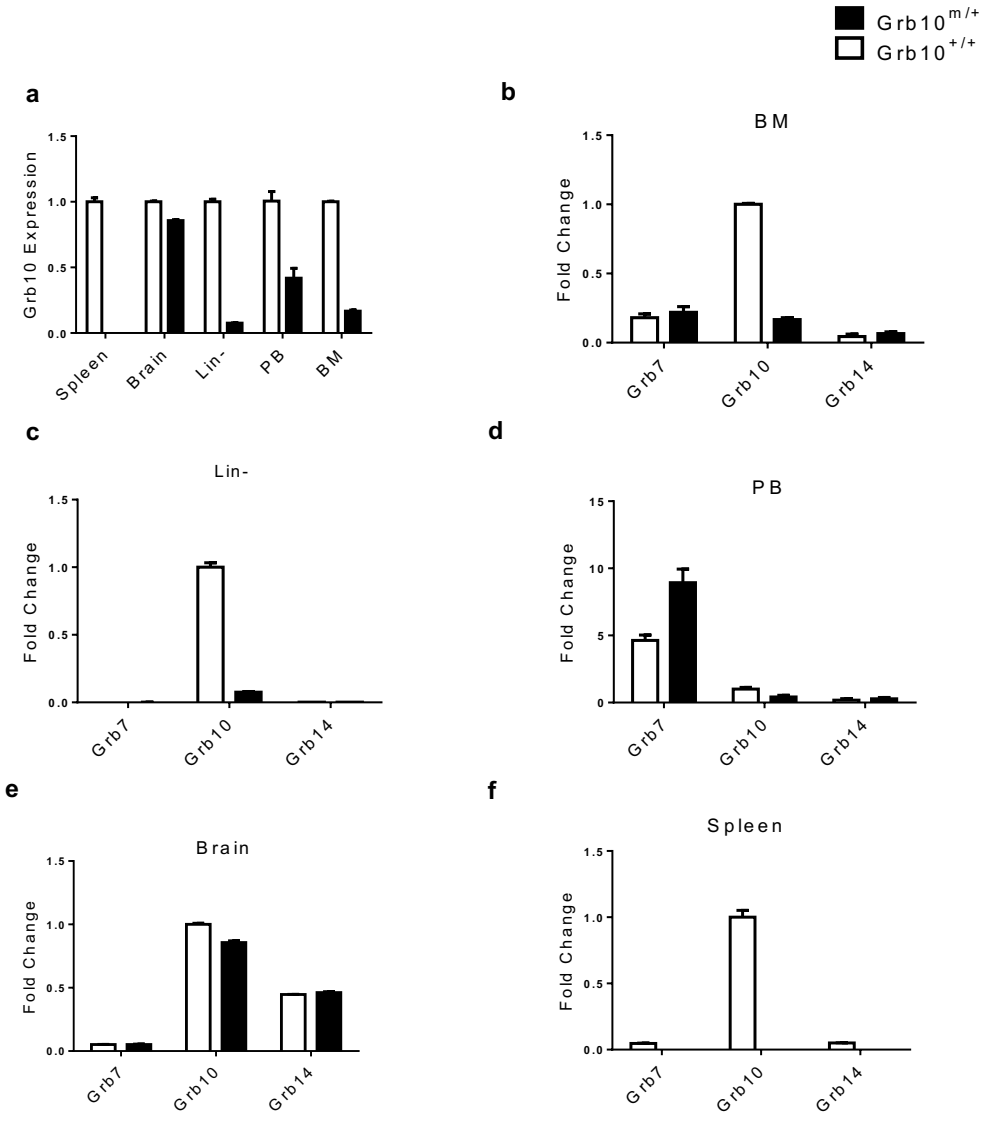

Figure 8 Expression of Grb family members in different organs in Grb10$^{m/+}$ mice

(a) qRT-PCR shows the expression of Grb10 in $Grb10^{+/+}$ and $Grb10^{m/+}$ mice in different tissues. (n = 3 mice / group) (b-f) qRT-PCR shows the expression of Grb7, Grb10, Grb14 in the $Grb10^{+/+}$ and $Grb10^{m/+}$ mice in (b) BM, (c) $lineage^{-}$ cells, (d) PB, (e) Brain, and (f) Spleen. (n = 3 mice / group)

First, we performed complete blood count (CBC) assay to determine whether ablation of Grb10 shows any effect on peripheral blood (PB). Adult $Grb10^{m/+}$ mice displayed moderately increased peripheral blood WBCs, hemoglobin, platelet counts compared to $Grb10^{+/+}$ mice (**Figure 9**). However, no differences were observed in spleen sizes compared to $Grb10^{+/+}$ littermates (Data not shown).

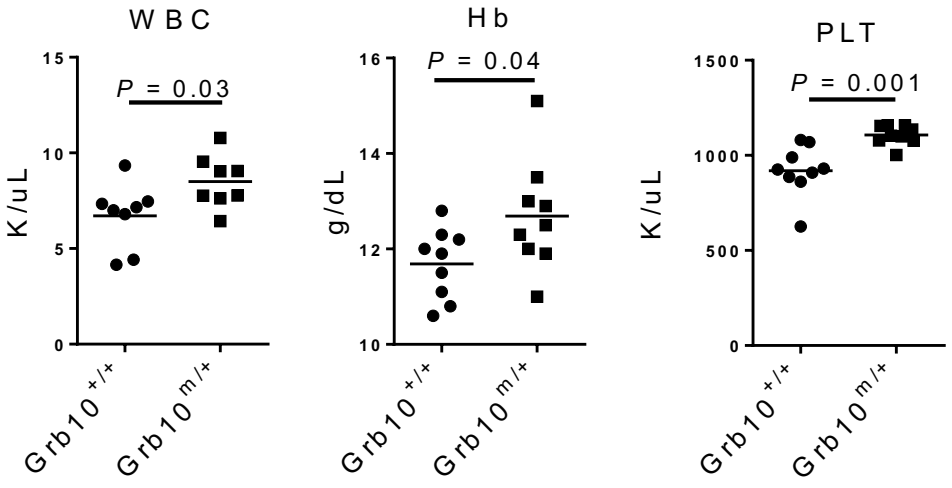

Figure 9 Complete blood counts (CBCs) of Grb10 maternal deletion mice

Complete blood counts of peripheral blood comparing $Grb10^{m/+}$ mice with $Grb10^{+/+}$ mice (n = 8 – 10 mice/group, t-tests).

We then stained lineage markers Mac-1/Gr-1, B220 and CD3 in the PB of $Grb10^{+/+}$ and $Grb10^{m/+}$ mice. In accordance with the previous data, $Grb10^{m/+}$ mice have higher percentage of Mac-1/Gr-1^{+} myeloid cells but not $B220^{+}$ B cells and $CD3^{+}$ T cells (**Figure 10**). Previous research suggests that Grb10 is highly expressed in the $CD71^{+}Ter119^{+}$ erythroid progenitors (EPs) and $lineage^{-}c\text{-}kit^{+}sca\text{-}1^{-}CD150^{+}CD41^{+}$ megakaryocyte progenitors (MkPs)[110], indicating a functional role of Grb10 in these progenitors. We performed BM analysis of the EPs and MkPs with $Grb10^{+/+}$ and $Grb10^{m/+}$ mice **(Figure 11**). Grb10 maternal deletion leads to increased percentage of both EPs and MkPs compared to $Grb10^{+/+}$ mice. These data further confirmed the myeloproliferative defect caused by Grb10 ablation.

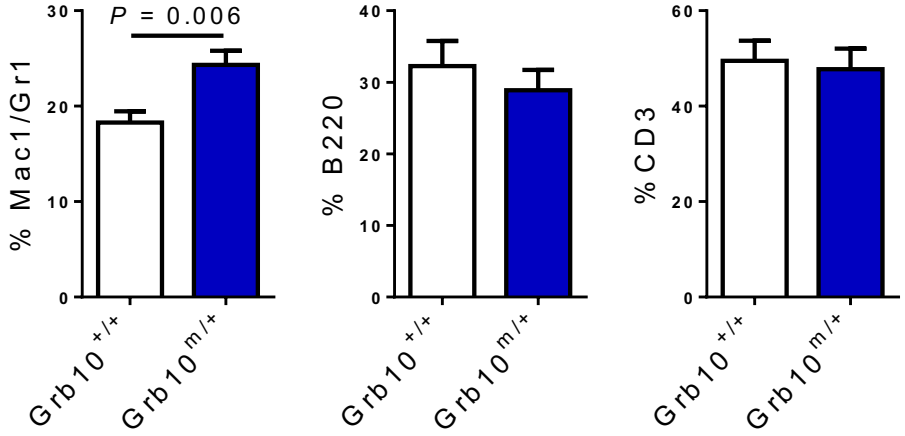

Figure 10 Lineage staining in the PB of $Grb10^{+/+}$ and $Grb10^{m/+}$ mice

Percentage of PB myeloid cells (Mac-1/Gr-1^{+}), B cells ($B220^{+}$) and T cells ($CD3^{+}$) in the PB of $Grb10^{m/+}$ mice and $Grb10^{+/+}$ mice (n = 8 mice/group).

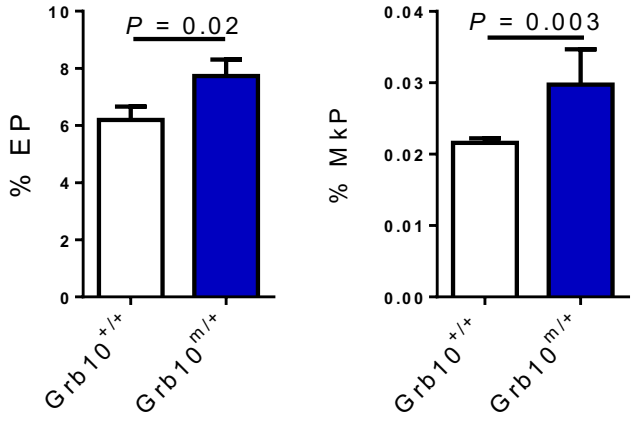

Figure 11 EPs and MkPs in the BM of Grb10$^{+/+}$ and Grb10$^{m/+}$ mice

Mean percentage of erythroid progenitors (EPs) and megakaryocyte progenitors (MkPs) in *Grb10*$^{m/+}$ mice and *Grb10*$^{+/+}$ mice (n=8/group).

To determine the effect of Grb10 ablation in BM cells, which is the primary organ for HSCs, we isolated BM cells from Grb10$^{+/+}$ or Grb10$^{m/+}$ mice and performed a series of hematologic assays. No significant differences were observed in BM cell counts. H&E staining of femurs from Grb10$^{+/+}$ and Grb10$^{m/+}$ mice confirmed no obvious difference was observed in cellularity (**Figure 12**). To further evaluate the change in phenotypic stem cells, we stain the BM for lineage^{-}c-kit^{+} sca-1^{+} (KSL) cells or CD150^{+}CD48^{-}KSL (SLAM KSL) cells which enrich for the long-term HSCs. Roughly one-third of the SLAM KSL cells were shown to have long-term repopulating capability. However, we did not observe any significant difference between Grb10$^{+/+}$ and Grb10$^{m/+}$ mice. These data indicate that Grb10 ablation at steady state did not influence phenotypic hematopoietic stem cells.

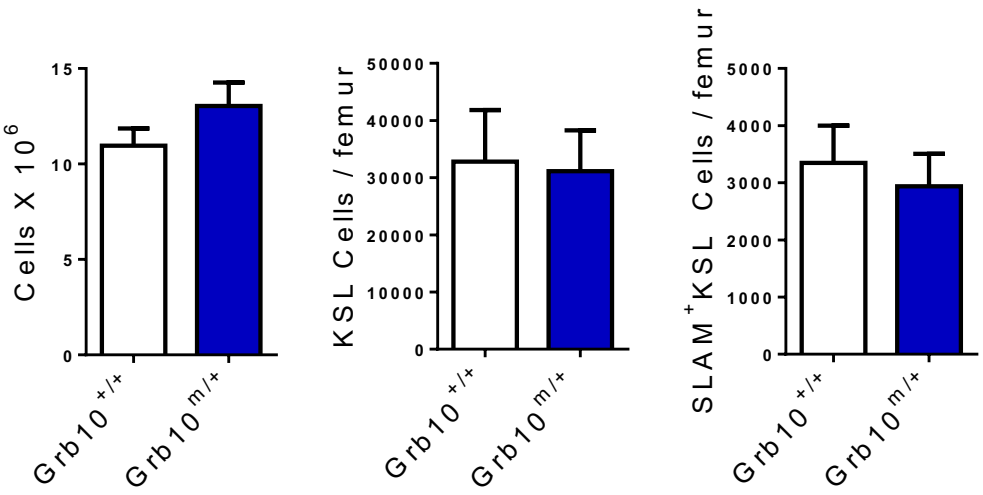

Figure 12 BM analysis of Grb10 maternal deletion mice

Left, BM counts of $Grb10^{+/+}$ and $Grb10^{m/+}$ mice (n = 8 mice / group). Middle and right, Percentage of KSL cells and $CD150^{+}$ $CD48^{-}$ KSL (SLAM KSL) cells of $Grb10^{+/+}$ mice and $Grb10^{m/+}$ mice were shown by flow cytometric analysis (n = 8 – 12 mice /group).

To test the hypothesis whether Grb10 ablation induces functional change in hematopoietic progenitors at steady state, we isolated whole bone marrow cells from $Grb10^{+/+}$ and $Grb10^{m/+}$ mice, and performed colony-forming-cells (CFCs) assay. $Grb10^{m/+}$ contained significantly increased BM colony forming cells (CFCs) (**Figure 13**). This data suggests that disruption of Grb10 expression mainly influence progenitors.

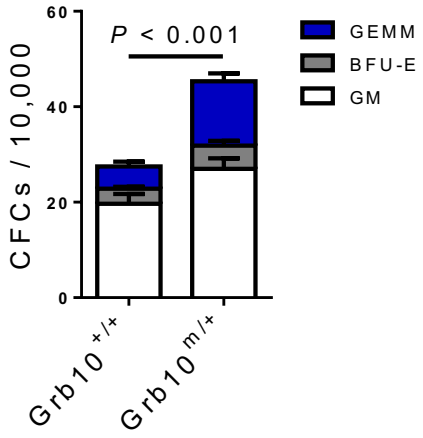

Figure 13 Colony forming cells assay of Grb10 maternal deletion bone marrow

Colony-forming cells (CFCs) with 10,000 BM cells of $Grb10^{+/+}$ and $Grb10^{m/+}$ mice. GEMM, granulocyte erythroid monocyte megakaryocyte; BFUE, burst-forming unit-erythroid; GM, granulocyte macrophage (n = 6 / group, t-test).

The gold standard to test the effect on hematopoietic stem cells is the competitive repopulating unit (CRU) assay. $CD45.2^{+}$ BM cells from $Grb10^{+/+}$ or $Grb10^{m/+}$ were mixed with a dose of competitor cells expressing cell surface marker $CD45.1^{+}$, and injected into lethally irradiated recipient mice. At 4, 8, 12, 16 and 20th week after BM transplantation, peripheral blood from recipient mice was sampled for donor engraftment. Although no significant difference was observed between $Grb10^{+/+}$ and $Grb10^{m/+}$ donor engraftment at 4^{th} week after transplantation, starting at 8^{th} week, mice transplanted with BM cells from $Grb10^{m/+}$ mice displayed significantly higher donor engraftments compared with mice transplanted with $Grb10^{+/+}$ cells. Specifically, at 20^{th} week post-transplant, mice transplanted competitively with BM cells from $Grb10^{m/+}$ mice displayed approximately 6-fold increased donor-derived, multilineage hematopoietic cell repopulation (**Figure 14**). Most importantly, this difference in donor engraftment capability is

multi-lineage, when we analyzed donor-derived Mac-1^+/Gr-1^+ myeloid cells, $CD3^+$ T cells and $B220^+$ B cells (**Figure 15**). Additionally, we did not observe lineage skewing in the donor derived mature cells (**Figure 16**). These data indicate Grb10 depletion promotes the engraftment capability of hematopoietic cells in a transplantation setting.

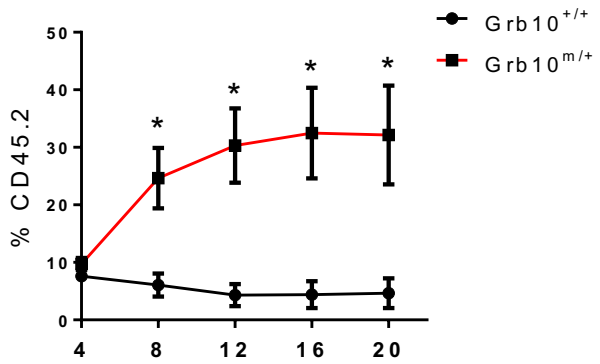

Figure 14 Time course of competitive bone marrow transplantation

Donor ($CD45.2^+$) cell engraftment over time in recipient $CD45.1^+$ mice transplanted with 100,000 BM cells from $Grb10^{+/+}$ and $Grb10^{m/+}$ mice, together with 200,000 $CD45.1^+$ competitor cells (n = 10 - 12 mice / group. p = 0.007, p = 0.01, p = 0.003, p = 0.005, for 8, 12, 16, 20 weeks, respectively, Mann-Whitney test). (h) PB analysis of donor derived $CD45.2^+$ cells in the primary recipient at 20 weeks after transplantation (Mann-Whitney test).

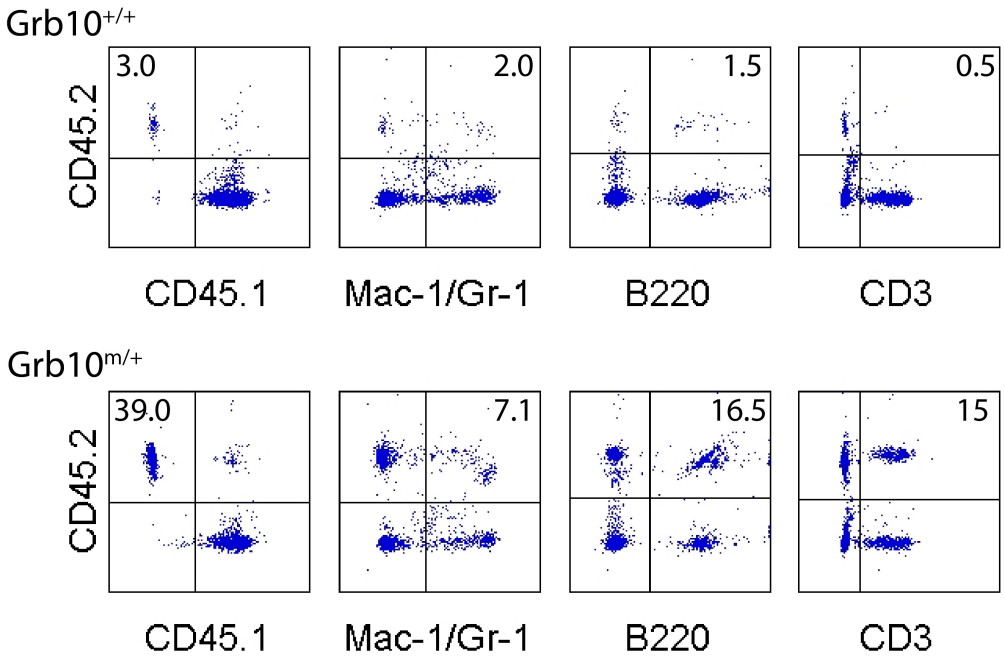

Figure 15 Representative flow cytometry plot of competitive bone marrow transplantation

Representative flow cytometric plot of data in Figure 14 at 20wks after bone marrow transplantation. Percentages of each cell populations are shown in the quadrants.

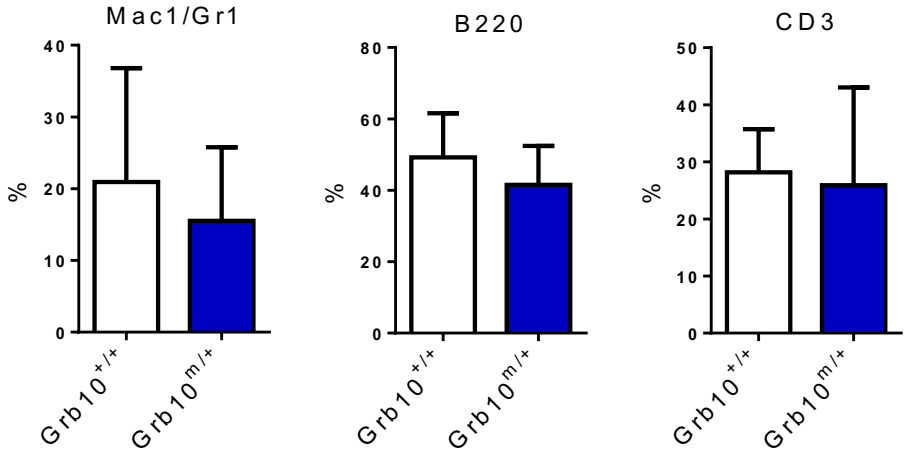

Figure 16 Lineage skewing analysis in the primary recipients of competitive bone marrow transplantation

Mean Mac-1/Gr-1^{+}, B220^{+} and CD3^{+} cells as a percentage of total engrafted donor cells in recipient mice transplanted with Grb10$^{+/+}$ and Grb10$^{m/+}$ donor cells, at 20 weeks in PB after primary bone marrow transplantation (n = 10-12 /group).

In order to determine the contribution of donor cells in different components of bone marrow cells in the recipients, we performed flow cytometry analysis of donor derived BM HSCs (CD150^{+}CD48^{-}Lineage^{-}Sca-1^{+}c-Kit^{+}), MPPs(CD150^{-}CD48^{-}Lineage^{-}Sca-1^{+}c-Kit^{+}), CMPs (CD34^{+}CD16/32^{low}CD127^{-}Lineage^{-}Sca-1^{-}c-Kit^{+}), GMPs(CD34^{+}CD16/32^{high}CD127^{-}Lineage^{-}Sca-1^{-}c-Kit^{+}), MEPs(CD34^{-}CD16/32$^{-/low}$CD127^{-}Lineage^{-}Sca-1^{-}c-Kit^{+}) cells (**Figure 17**). Recipient mice transplanted with Grb10$^{m/+}$ donor cells show significantly higher donor engraftment in the BM HSCs, MPPs and MEPs, a trend in the CMPs, but not in the GMPs. In order to confirm that the increase in engraftment capability can also be observed in the rare population of long-term HSCs, we performed secondary competitive repopulation assay in which we isolated and competitively transplanted BM cells from primary recipient mice and tail-vein injected into lethally irradiated secondary recipient mice. Secondary, competitive repopulation assays showed that Grb10$^{m/+}$ BM cells contained significantly increased, long-term multilineage repopulating capacity compared to Grb10$^{+/+}$ mice (**Figure 18**). This difference is not significant at 4th week after bone marrow transplantation, but increases with time and at 20th week, mice transplanted with Grb10$^{m/+}$ cells show a significant 8-fold increase in the donor engraftment. Again, we found significant difference in all of the lineage-derived donor cells in the Grb10$^{m/+}$ group compared to Grb10$^{+/+}$ group. These data suggest that deletion of Grb10 causes a substantial increase in HSC long-term repopulating capacity.

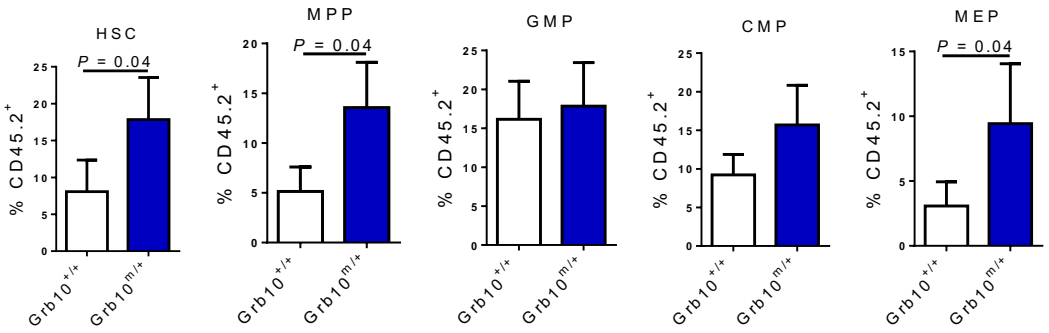

Figure 17 BM analysis of donor derived HSCs, MPPs, GMPs, CMPs and MEPs in the primary recipient mice of competitive bone marrow transplantation

Mean donor-derived HSCs, MPPs, CMPs, GMPs and MEPs in the BM of recipient mice following competitive transplantation (n=8/group).

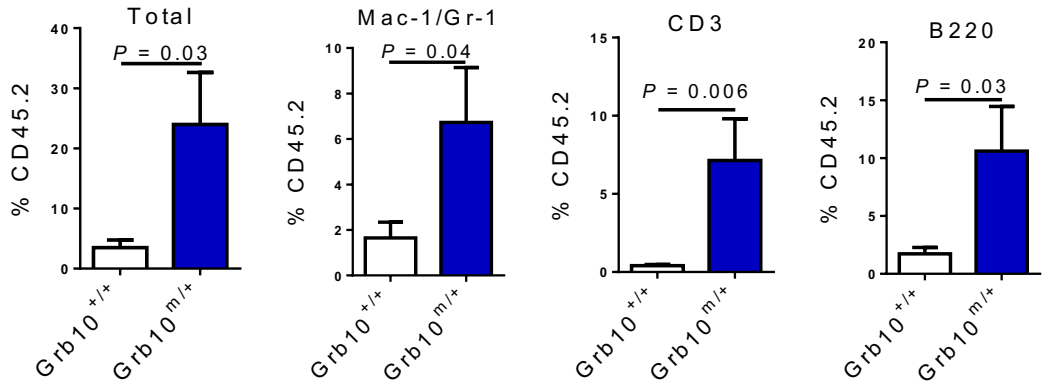

Figure 18 Secondary bone marrow transplantation

PB analysis of donor derived CD45.2^{+} cells in the secondary recipient mice, transplanted with bone marrows isolated from primary recipient mice in (h), at 8 weeks after secondary transplantation (n = 10 mice / group, Mann-Whitney test).

2.3 Maternal deletion of Grb10 promotes HSC regeneration following TBI

2.3.1 Methods

Immunohistochemistry Hematoxylin and eosin (H&E) staining of femurs from mice was performed as previously described[40]. Images were obtained using an Axiovert 200 microscope (Carl Zeiss, Thornwood, NY).

Flow cytometric analysis BM cells were collected from tibias and femurs and stained with anti-c-kit APC-Cy7 (BD Biosciences), anti-Sca-1 PE (BD Biosciences), anti-lineage V450 (BD Biosciences), anti-CD48 FITC (Biolegend), and anti-CD150 Alexa Fluor 647 (Biolegend). Flow cytometric analysis was performed on a FACS CANTO II (BD Biosciences).

Mouse competitive repopulation assays. 10-12-week-old $Grb10^{m/+}$ mice and $Grb10^{+/+}$ mice which express CD45.2 was irradiated with a Cesium 137 irradiator for a single dose of 550cGy. Mouse BM cells were isolated from $Grb10^{m/+}$ mice and $Grb10^{+/+}$ mice. Ten-week old recipient $CD45.1^{+}$ B6.SJL mice were irradiated with 950cGy TBI 12 hours prior to transplantation. At day+10 following irradiation, BM cells (5×10^5) from $Grb10^{m/+}$ mice or $Grb10^{+/+}$ mice were injected via tail vein into recipient mice along with 1×10^5 host competitor BM cells. Multilineage hematopoietic cell engraftment was measured by flow cytometric analysis of the PB every 4 weeks through week 20 post-transplant, as previous described[23,40]. For secondary competitive repopulation assays, BM cells from primary recipient mice were injected via tail vein into irradiated B6.SJL mice with 2×10^5 host competitor BM cells from the B6.SJL mice. Donor hematopoietic cell engraftment was measured by flow cytometry at 4 through 20 weeks posttransplant.

Colony-forming-cell (CFC) assay. BM cells from $Grb10^{m/+}$ and $Grb10^{+/+}$ mice were flushed out from the hinder bones (tibias and femurs) by a 25-gauge needle with 1X DPBS plus 10% FBS, 1% penicillin-streptomycin. Cells were counted with an automatic cell counter (Bio-rad). 10,000

cells from Grb10$^{m/+}$ or Grb10$^{+/+}$ mice were resuspended in methylcellulose methocult M3434 (STEMCELL Technologies) and plated into a 35mm dish with grid. Cells were cultured in an incubator at 37°C for 14 days and counted based on the instructions on the datasheet.

2.3.2 Results

Since the expression of Grb10 increased in HSCs during recovery from TBI, we sought to determine if Grb10 regulated HSC regeneration in mice. Grb10$^{m/+}$ mice or Grb10$^{+/+}$ mice were irradiated at 550cGy. At day+10 after irradiation, which is potentially the regenerative phase after irradiation, hinder bones from Grb10$^{m/+}$ and Grb10$^{+/+}$ mice were sampled and stained with H&E. As shown in **Figure 19**, Grb10$^{m/+}$ mice show significantly increased cellularity compared to Grb10$^{+/+}$. And whole bone marrow counts confirmed a significant increase in cellularity in Grb10$^{m/+}$ mice compared to Grb10$^{+/+}$ mice.

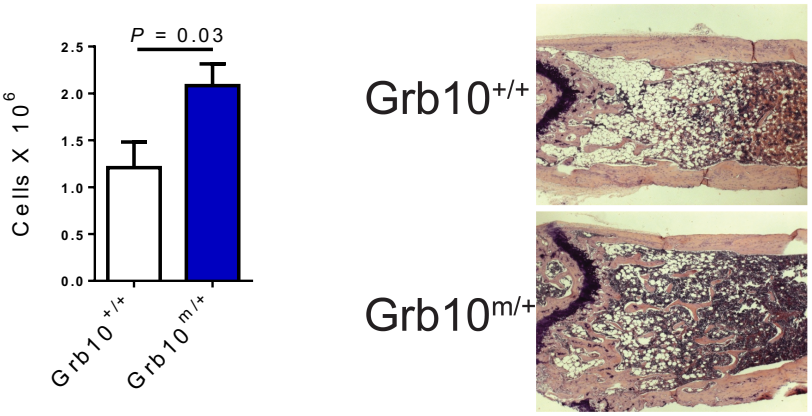

Figure 19 BM cellularity recovery of Grb10 maternal deletion mice after total body irradiation

Left, BM counts of Grb10$^{+/+}$ and Grb10$^{m/+}$ mice at day+10 following 550cGy irradiation (n = 6 mice / group, t-test). Right, H&E stained femurs of upper, Grb10$^{+/+}$ mice and lower, Grb10$^{m/+}$ mice at day+14 following 550cGy irradiation. Pictures are representatives of 3 – 5 femurs.

To determine if Grb10 deletion accelerates the regeneration of hematopoietic progenitors after irradiation, we performed colony-forming-cell (CFC) assay at day+10 and day+14 after 550cGy. Surprisingly, Grb10 deletion promotes the recovery of CFCs both at day+10 and day+14 after irradiation (**Figure 20**). Numbers of both KSL and $SLAM^{+}$ KSL cells were significantly higher in the $Grb10^{m/+}$ mice compared to $Grb10^{+/+}$ mice, indicating that the deletion of Grb10 accelerates the regeneration of phenotypic HSCs after irradiation (**Figure 21**).

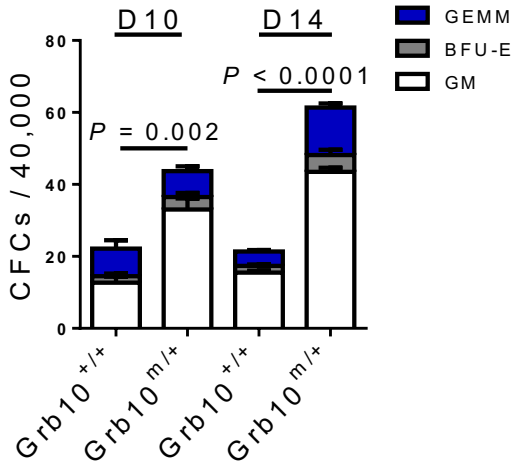

Figure 20 Colony forming cells of Grb10 maternal deletion mice after total body irradiation

BM CFCs using 40,000 BM cells of $Grb10^{+/+}$ and $Grb10^{m/+}$ mice, at day+10 and day+14 following 550cGy irradiation (n = 6 / group, t-test).

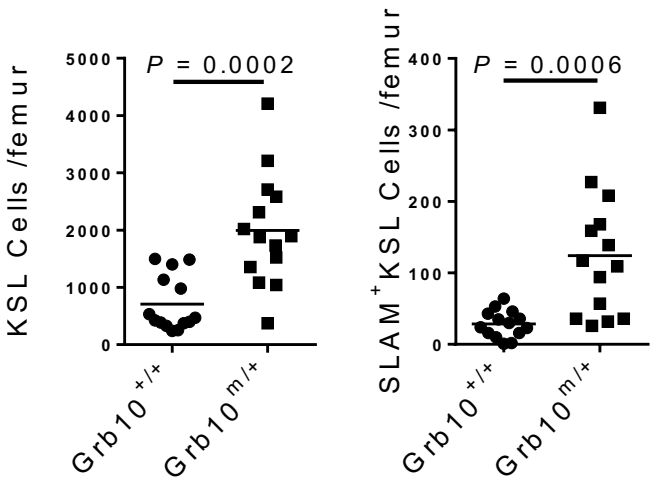

Figure 21 BM KSL and SLAM KSL staining of Grb10 maternal deletion mice

Scatter plot shows the percentage of left, KSL and right, SLAM KSL cells in $Grb10^{+/+}$ and $Grb10^{m/+}$ mice at day+10 following 550cGy irradiation (n = 12 – 14 mice /group, t-test).

We then performed competitive transplantation experiment to determine the effect on HSC regeneration in $Grb10^{m/+}$ mice versus $Grb10^{+/+}$ mice. Mice that were competitively transplanted with BM cells collected at day +10 from irradiated, $Grb10^{m/+}$ mice displayed approximately 8-fold higher donor hematopoietic cell repopulation post-transplant compared to mice transplanted with BM cells from identically irradiated, $Grb10^{+/+}$ mice (**Figure 22**). This difference in donor engraftment is persistent until 20wks in the primary recipient mice. Again, we observed increase of engraftment in all of the donor-derived lineages in the recipient mice (**Figure 23**). Data from secondary BM transplantation show a trend that $Grb10^{m/+}$ deletion promotes the regeneration of long-term HSCs, but more data will be needed to assess whether this trend is significant. These results suggested that deletion of Grb10 accelerated the regeneration of long-term repopulating HSCs and progenitor cells following TBI.

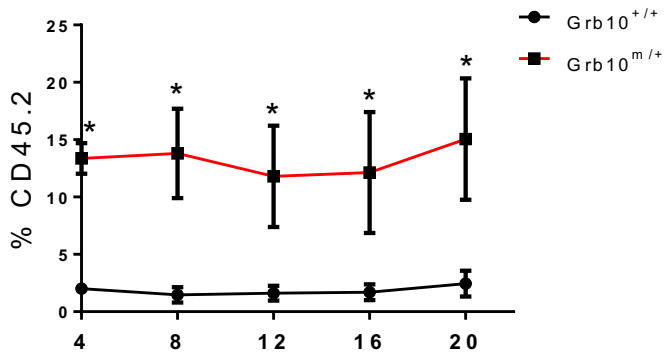

Figure 22 Time course of competitive bone marrow transplantation with irradiated Grb10$^{m/+}$ donor cells

Grb10$^{+/+}$ and Grb10$^{m/+}$ mice were irradiated at 550cGy and BM cells were isolated at day+10. 500,000 irradiated BM cells were transplanted into lethally irradiated mice together with 100,000 CD45.1^{+} competitor BM cells. Scatter plot shows the PB analysis of donor derived CD45.2^{+} cells in the primary recipient mice at 20 weeks after transplantation (n = 8 – 10 mice /group, Mann-Whitney test).

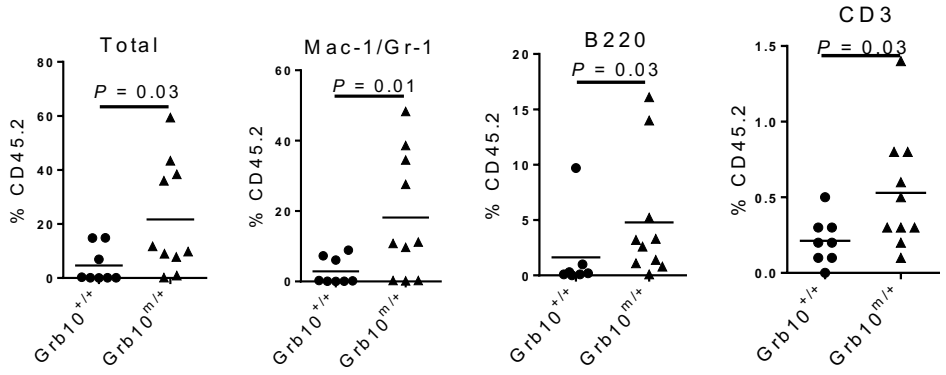

Figure 23 Representative flow cytometry plot of competitive bone marrow transplantation with Grb10 maternal deletion cells

Donor ($CD45.2^+$) cell engraftment over time in recipient $CD45.1^+$ mice in (e) (n = 8 -10 mice / group. p = 0.01, p = 0.001, p = 0.008, p = 0.03, for 8, 12, 16, 20 weeks, respectively, Mann-Whitney test).

2.4 Grb10 deletion increases stem/progenitor cell proliferative potential and migratory capacity

2.4.1 Methods

Statistics. Unless stated otherwise in the Figure Legends, all graphical data are presented as means + s.e.m., except histograms, and significance was calculated using two-tailed Student's t test. $P < 0.05$ was considered significant. Competitive repopulating assays were compared with a two-tailed Mann-Whitney test. For all animal studies, we used a power test to determine the sample size needed for a 2-fold difference in mean with 0.8 power using a two-tailed Student's t-test. Animals in our studies were sex and age-matched and littermates were used as controls.

Mice. All mouse procedures were performed in accordance with UCLA animal research and oversight committee-approved protocols. Grb10Δ2-4 mice were a kind gift from Dr. Andrew Ward (University of Bath, UK). Grb10Δ2-4 mice were extensively backcrossed into a C57BL/6 background for these studies. $Grb10^{m/+}$ mice, $Grb10^{+/+}$ mice and $Grb10^{+/p}$ mice were evaluated at 8-12 weeks of age. C57BL/6 mice and B6.SJL mice between 8-12 weeks old were obtained from the Jackson Laboratory (Bar Harbor, ME).

BrdU incorporation, cell cycle analysis and Annexin V analysis. For short-term analysis, $Grb10^{m/+}$ mice or $Grb10^{+/+}$ mice were injected intraperitoneally with 2mg BrdU suspended in PBS. At 24 hours, BM cells were collected and stained with FITC BrdU (BD). For longer term BrdU incorporation assay, BrdU was added into the drinking water of mice to a concentration of

1mg/ml and replaced every 72 hours. After 14 days, BM cells of the mice were isolated and stained with FITC BrdU.

For cell cycle analysis, BM cells were flushed into PBS plus 10% FBS and stained for surface c-kit, sca-1 and lineage markers for 30 minutes. Cells were then fixed with buffer (BD) for 30 minutes, followed by incubation of permeabilization buffer (BD). Anti-Ki67 FITC (BD) was added to the cells and incubated for 30 minutes. 7AAD was added to stain for DNA content.

For analysis of HSC apoptosis in $Grb10^{m/+}$ mice or $Grb10^{+/+}$ mice, BM cells were stained with anti c-kit, anti-sca-1 and anti-lineage antibodies for 30 minutes, followed by application of the FITC Annexin V Apoptosis Detection Kit I (BD), as previously described[23].

Homing Assay. 2 x 10^4 BM Sca-1^+Lin$^-$ cells ($CD45.2^+$) were injected into lethally irradiated B6.SJL recipients ($CD45.1^+$) and donor cell engraftment was measured by flow cytometry at 18 hours after transplant, as previously described[23].

Transendothelial migration assay. Murine spleen ECs (Angiocrine Bioscience, New York, NY) were cultured on 8.0 μM pore transwells (Corning Incorporated) until confluent. BM cells (2 x 10^5) were seeded onto the transwell and inserted into a 24-well plate, as previously described[23]. 100ng/ml SDF-1 (R&D Systems) was added to the bottom chamber of the plate. After 16 hours, cells in the bottom chamber were collected and counted with an automated cell counter (Bio-Rad). Cells from the bottom chamber (5 x 10^3) were placed in MethoCult M3434 medium for 14-day CFC assay.

2.4.2 Results

Since Grb10-deficient HSCs displayed increased self-renewal capacity following competitive transplantation and following radiation injury, we sought to determine the cellular mechanism responsible for these effects. To examine the cell cycle status of the $Grb10^{m/+}$ and $Grb10^{+/+}$ mice,

we injected the mice with BrdU to mark proliferating HSCs, and stained for $BrdU^+$ cells at 24h after BrdU injection. We observed no differences in HSC proliferation between $Grb10^{m/+}$ mice and $Grb10^{+/+}$ mice in steady state (**Figure 24**). We also stained $Grb10^{m/+}$ and $Grb10^{+/+}$ KSL cells with anti-Ki67 and 7AAD, and observed no differences in cells at G0, G1 or S/G2/M phase. To analyze the cell death profile, BM cells from $Grb10^{m/+}$ and $Grb10^{+/+}$ mice were stained with Annexin V and 7AAD. Without injury, $Grb10^{m/+}$ and $Grb10^{+/+}$ mice show similar percentage of dead cells in the BM. At 24 hours following 700 cGy TBI, we also observed no difference in BM KSL cell survival between $Grb10^{m/+}$ mice and $Grb10^{+/+}$ mice.

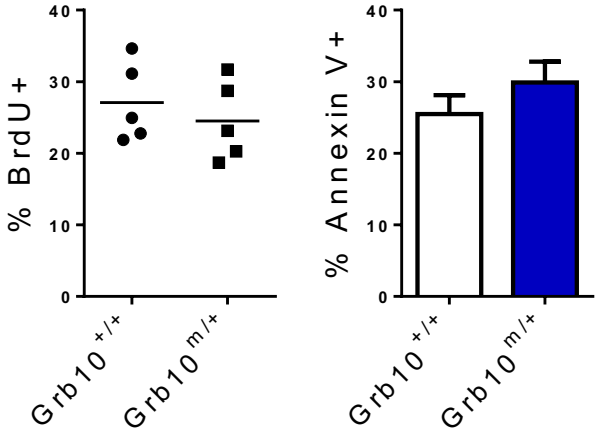

Figure 24 Cell proliferation and cytotoxicity assay of Grb10 maternal deletion mice at homeostasis

Left, percentage of $BrdU^+$ KSL cells in the $Grb10^{+/+}$ BM and $Grb10^{m/+}$ BM (n = 5 mice / group). Right, percentage of Annexin V^+ KSL cells in the $Grb10^{+/+}$ BM and $Grb10^{m/+}$ BM (n = 8 mice / group).

At homeostasis, Grb10 deficiency did not influence the phenotypic HSCs. However, after irradiation damage and in the transplantation model, which is also related to injury related stress,

Grb10 ablation promotes the recovery of HSCs and elevates the engraftment percentage. These observations lead us to hypothesize that the effect of Grb10 ablation on HSC cell proliferation can only be observed under stress setting. To test our hypothesis, B6 mice were lethally irradiated and transplanted with whole BM cells from $Grb10^{m/+}$ or $Grb10^{+/+}$ mice. At 48 hours following transplantation, we observed significantly increased BrdU incorporation in transplanted $Grb10^{m/+}$ cells in the BM of recipient mice compared to $Grb10^{+/+}$ BM cells (**Figure 25**). These data suggested that Grb10 deletion primed transplanted BM cells to proliferative more rapidly following homing to the BM niche.

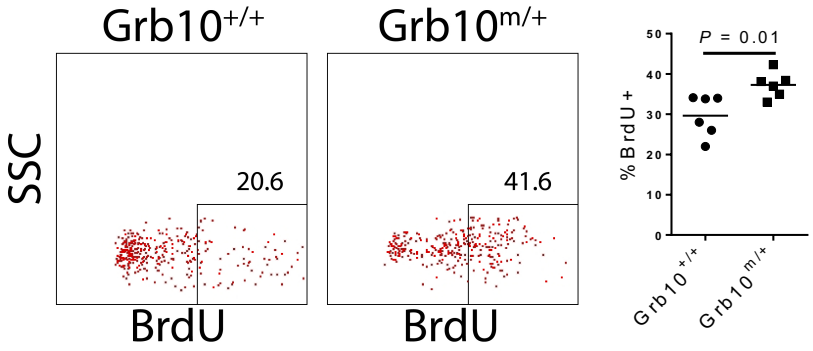

Figure 25 BrdU incorporation of Grb10 after bone marrow transplantation

At left, representative flow cytometric plots are shown of BrdU positive donor $CD45.1^+$ BM cells at 48 hours following transplantation of BM cells from *Grb10*$^{+/+}$ mice and *Grb10*$^{m/+}$ mice into $CD45.2^+$ recipients. At right, the scatter plot shows the mean percentage of BrdU positive BM cells in each group (n=6/group).

In a radiation injury model, we found that an increased percentage of BM KSL cells in $Grb10^{m/+}$ mice had entered G1 and S/G2/M phase at 24 hours after 700cGy TBI compared to BM KSL cells in $Grb10^{+/+}$ mice (**Figure 26**). In a comparable study, at 1h after 300cGy in vitro irradiation, $Grb10^{m/+}$ KSL cells have a greater trend to transit from G1 to S/G2/M active cell cycle (**Figure**

27). Concordantly, the expression of several cyclin dependent kinases (CDKs) and cyclin proteins, CDK4 and CyclinE, was significantly decreased in Grb10$^{m/+}$ BM KSL cells compared to Grb10$^{+/+}$ BM KSL cells (**Figure 28**). However, the expression of several well-known CDK inhibitors, including p16, p18, p27 and p57, have shown no difference in expression level in Grb10$^{m/+}$ mice compared to Grb10$^{+/+}$ mice, suggesting a unique mechanism that happens in CDK and cyclin level. P16 is known to be a critical marker for cell senescence[111]. In accordance with this, percentages of senescence associated-β galactosidase positive CD34^{-}KSL cells were comparable in Grb10$^{+/+}$ and Grb10$^{m/+}$ mice (**Figure 29**). Taking all the data into consideration, Grb10 ablation promotes HSC proliferation by regulating cell cycle under irradiation stress.

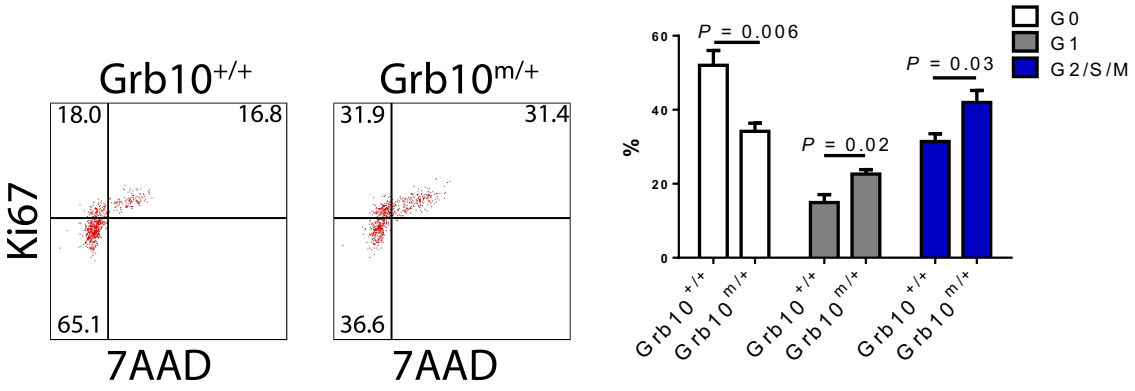

Figure 26 Cell cycle analysis in the Grb10$^{m/+}$ and Grb10$^{+/+}$ mice

At left, representative cell cycle analysis of BM c-kit^{+}sca-1^{+}lin^{-} cells at 24 hours following 700cGy in *Grb10$^{m/+}$* mice and *Grb10$^{+/+}$* mice. At right, mean percentages of cells in G_0, G_1 and G_2/S/M phase in each group (n=4 mice/group).

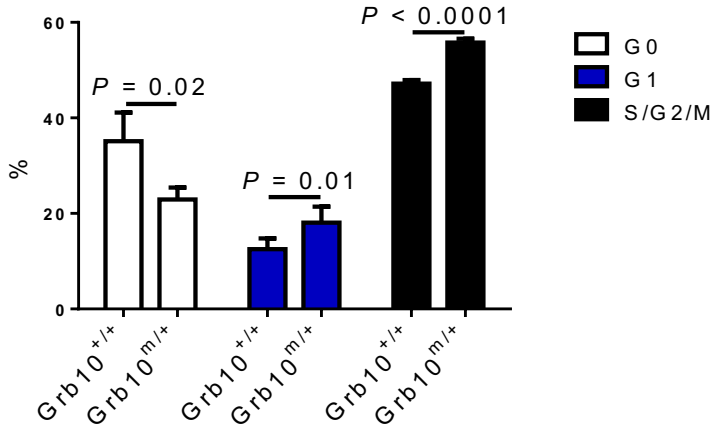

Figure 27 Cell cycle analysis of Grb10$^{+/+}$ and Grb10$^{m/+}$ KSL cells at 3h after 300cGy in vitro irradiation

Mean percentages of Grb10$^{+/+}$ and Grb10$^{m/+}$ KSL cells in G_0, G_1 and G_2/S/M phase at 3h after 300cGy in vitro irradiation (n = 6 / group).

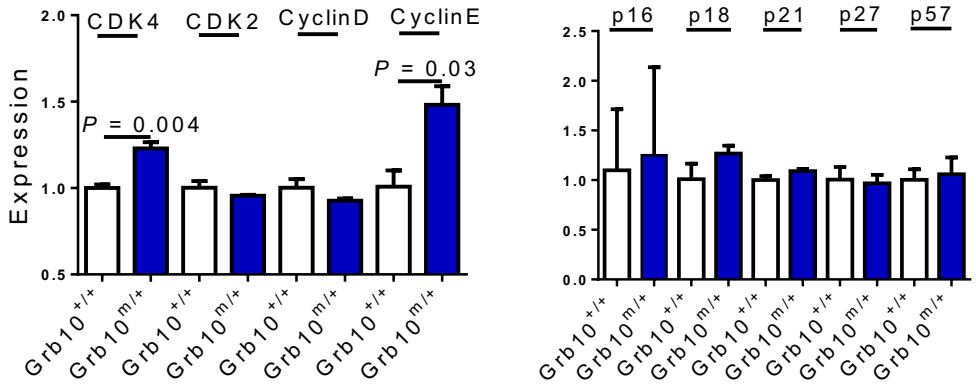

Figure 28 Expression of molecular markers after 300cGy in vitro irradiation

qRT-PCR analyses of cell cycle regulators in BM lineage$^-$ cells of Grb10$^{+/+}$ and Grb10$^{m/+}$ mice, at 6h after 300cGy in vitro irradiation (n = 6 / group, t-test).

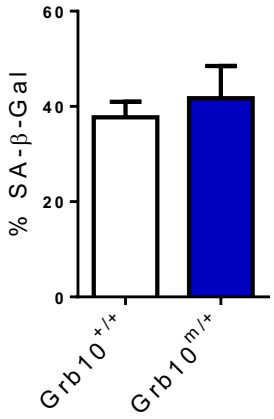

Figure 29 Senescence assay with CD34-KSL cells in Grb10$^{+/+}$ and Grb10$^{m/+}$ mice

Mean percentages of senescence associated-β-galactosidase positive cells within CD34^{-}KSL population, in Grb10$^{+/+}$ and Grb10$^{m/+}$ mice. (n = 8/group).

It is well established that during transplantation, HSCs in the circulation system need to migrate across the endothelial cells and homing to the stem cell niche in the bone marrow. During this process extracellular cytokines such as SDF-1 serves as a chemoattractant and guide homing of HSCs. Difference in the migration or homing capacity in the Grb10m/+ mice may explain the increase donor engraftment phenotype. We observed no difference in the homing capacity of transplanted Grb10$^{m/+}$ BM cells compared to Grb10$^{+/+}$ BM cells (**Figure 30**). In a transendothelial migration assay, we also observed significantly increased migration of Grb10$^{m/+}$ BM progenitor cells across endothelial cell monolayers toward an SDF1 gradient compared to Grb10$^{+/+}$ BM progenitor cells. These results suggested that deletion of Grb10 augmented HSC proliferative potential during the regenerative stress of BM transplantation and also increased their migratory capacity.

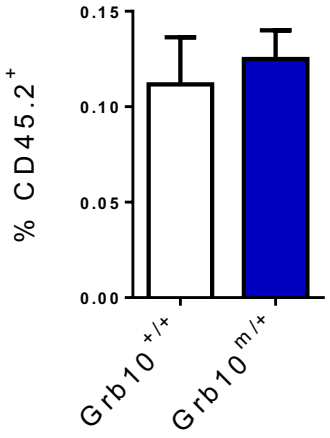

Figure 30 Homing assay using sca-1+lin- cells of Grb10$^{+/+}$ and Grb10$^{m/+}$ mice

Mean levels of donor CD45.2^{+} cells detected at 18 hours following transplantation of BM sca-1^{+}lin^{-} cells from *Grb10*$^{+/+}$ mice and *Grb10*$^{m/+}$ mice in recipient CD45.1^{+} mice (n=6/group).

2.5 Maternal deletion of Grb10 augments HSC regenerative capacity via activation of Rac1

2.5.1 Methods

Rac1 GTP assay. BM lin- cells from Grb10$^{m/+}$ mice and Grb10$^{+/+}$ mice were collected into PBS plus 1% FBS, 1% penicillin-streptomycin. Rac1 GTP was measured using the Rac1 G-Lisa Activation Assay Kit (Cytoskeleton, Inc., Denver, CO).

Transendothelial migration assay. Murine spleen ECs (Angiocrine Bioscience, New York, NY) were cultured on 8.0 μM pore transwells (Corning Incorporated) until confluent. BM cells (2 x 10^{5}) were seeded onto the transwell and inserted into a 24-well plate, as previously described[23]. For EHT1864 treatment, EHT1864 was directly put into the insert of the transwells. 100ng/ml SDF-1 (R&D Systems) was added to the bottom chamber of the plate. After 16 hours, cells in the bottom chamber were collected and counted with an automated cell counter (Bio-Rad). Cells from the bottom chamber (5 x 10^{3}) were placed in MethoCult M3434 medium for

14-day CFC assay.

2.5.2 Results

Since maternal deletion of Grb10 increased the proliferative potential and migratory capacity of BM stem/progenitor cells, we hypothesized that Grb10 deletion might be affecting the activity of Rac proteins, small RhoGTPases which have been shown to regulate HSC migration and proliferation[74,112]. RhoGTPases have been shown to be essential for mitogen-induced cell cycle progression through G1[113,114] in a p21-activated kinase (PAK)-dependent manner[114]. Rac1 and Rac2 have also been shown to be essential for the proper lodgment of transplanted hematopoietic stem/progenitor cells in the BM microenvironment[74,112].

We found that Rac1 GTP levels were significantly increased in $Grb10^{m/+}$ BM lin- cells at baseline and induced further following 700cGy TBI (**Figure 31**). Furthermore, the addition of EHT1864, a Rac inhibitor, abrogated the enhanced migratory capacity of $Grb10^{m/+}$ progenitor cells across endothelial cell monolayers (**Figure 32**). These data suggest an involvement of Rac1 in the migration assay. To determine if Rac1 regulates cell proliferation in the HSCs, we performed Ki-67 and 7AAD staining, in the conditions of with or without EHT1864 treatment. Systemic treatment with EHT1864 also abolished the increased cell cycle progression of $Grb10^{m/+}$ BM c-kit+sca1+lin- cells in vivo at 24 hours following TBI (**Figure 33**). In a separate study, overexpression of Rac1 in KSL cells with a lentivirus dramatically increases the hematopoietic progenitors in vitro (**Figure 34**). These results suggested that the enhanced proliferative potential and migratory capacity of Grb10-deficient hematopoietic stem/progenitor cells was dependent on Rac activation.

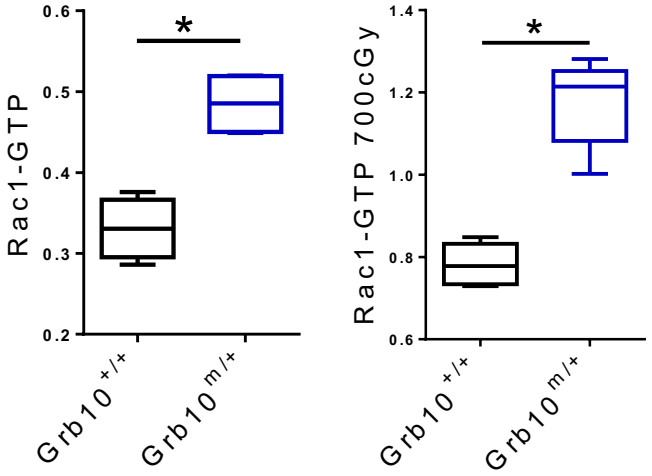

Figure 31 Rac1 activation assay in Grb10$^{+/+}$ and Grb10$^{m/+}$ mice

Mean Rac1-GTP positive BM lin$^-$ cells in non-irradiated *Grb10$^{m/+}$* mice and *Grb10$^{+/+}$* mice (left) and at 6 hours following 700 cGy TBI (right; n=4/group).

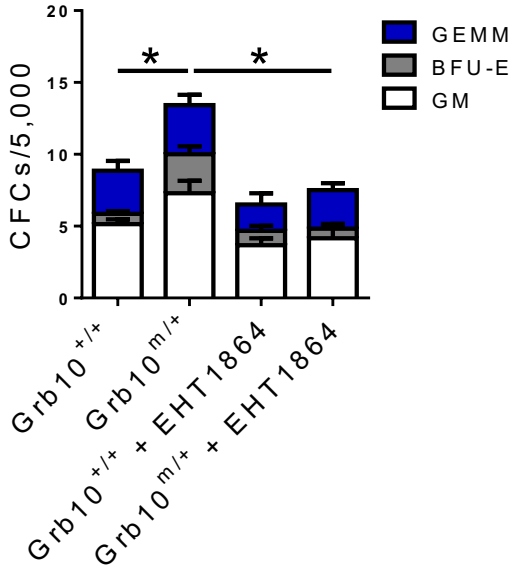

Figure 32 migration assay using whole bone marrow cells of Grb10$^{+/+}$ and Grb10$^{m/+}$ mice

Mean numbers of CFCs in the lower chambers of transendothelial migration assays of BM cells isolated from *Grb10*$^{+/+}$ mice and *Grb10*$^{m/+}$ mice and treated with and without EHT1864 (n = 5 - 6/group).

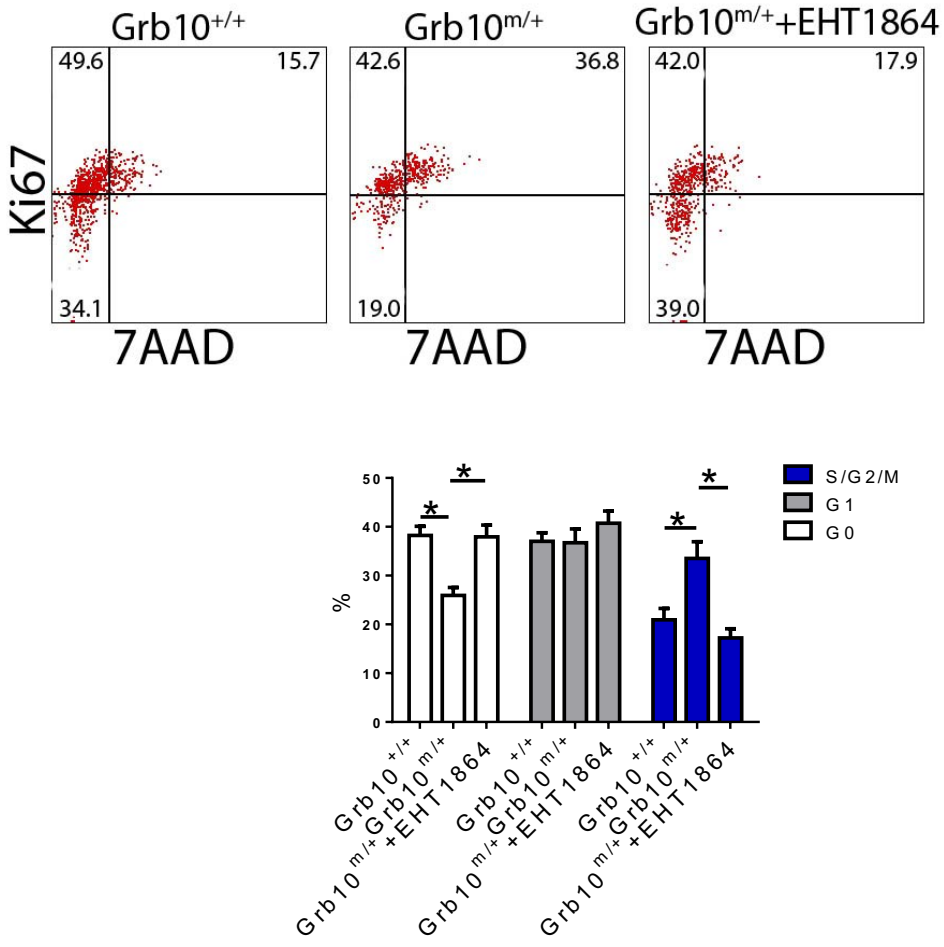

Figure 33 Ki67 and 7AAD analysis of Grb10$^{+/+}$ and Grb10$^{m/+}$ mice

At left, representative cell cycle analysis of BM c-kit^{+}lin^{-} cells in *Grb10*$^{m/+}$ mice and *Grb10*$^{+/+}$ mice at 24 hours following 700 cGy TBI and treated with or without EHT1864. At right, mean percentages of BM c-kit^{+}lin^{-} cells in G_0, G_1, and G_2/S/M phase are shown (n=6/group).

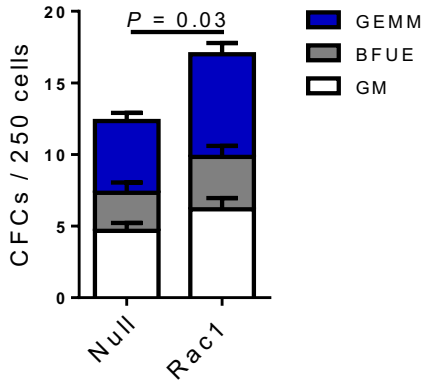

Figure 34 Rac1 overexpression assay with KSL cells

Mean number of CFCs set up with KSL cells infected with scramble virus or Rac1-expression virus (n = 6/ group).

2.6 Grb10 deletion potentiates mTOR activation in response to irradiation or SCF

2.6.1 Methods

Statistics. Unless stated otherwise in the Figure Legends, all graphical data are presented as means + SEM, except histograms, and significance was calculated using two-tailed Student's t test. $P < 0.05$ was considered significant. Competitive repopulating assays were compared with a two-tailed Mann-Whitney test. For all animal studies, we used a power test to determine the sample size needed for a 2-fold difference in mean with 0.8 power using a two-tailed Student's t-test. Animals in our studies were sex and age-matched and littermates were used as controls.

Flow cytometric analysis. BM cells were collected from tibias and femurs and stained with anti-c-kit APC-Cy7 (BD Biosciences), anti-Sca-1 PE (BD Biosciences), anti-lineage V450 (BD Biosciences), anti-CD48 FITC (Biolegend), and anti-CD150 Alexa Fluor 647 (Biolegend). For intracellular phosphoprotein analysis, BM cells were flushed into serum-free PBS. BM cells were stained with surface marker antibodies, then washed with PBS and fixed for 15mins at 4°C,

followed by incubation with BD cytoperm buffer for 30min at room temperature. Anti-pS6 PE (pSer235/236) or anti-pS6K PE (Thr389) (Cell Signaling Technology) or anti-pAkt PE (Cell Signaling Technology) were added at 1:50 dilution for 30mins. Flow cytometric analysis was performed on a FACS CANTO II (BD Biosciences).

Rac1 GTP assay and mTOR inhibition studies. BM lin- cells from $Grb10^{m/+}$ mice and $Grb10^{+/+}$ mice were collected into PBS plus 1% FBS, 1% penicillin-streptomycin. Rac1-GTP was measured using the Rac1 G-Lisa Activation Assay Kit (Cytoskeleton, Inc., Denver, CO). For mTOR inhibition studies, BM cells from $Grb10^{m/+}$ mice and $Grb10^{+/+}$ mice were collected into 1X IMDM plus 1% FBS, 1% penicillin-streptomycin, 20ng/ml thrombopoietin, 125ng/ml SCF, and 50ng/ml Flt-3 ligand. Cells were treated with 25 μM rapamycin (Selleckchem, Houston, TX) or vehicle for 24 hours and subsequently analyzed via the Rac1 G-Lisa assay.

For in vivo inhibition of mTOR, rapamycin (Selleckchem) was reconstituted in ethanol at 10mg/ml and then diluted in 5% Tween-80 (Sigma-Aldrich) and 5% PEG (polyethylene glycol) 400 (Hampton Research). $Grb10^{m/+}$ mice and $Grb10^{+/+}$ mice were irradiated at 550cGy at day+0, then injected with rapamycin (4mg/kg intraperitoneally) or vehicle every other day through day+10. At day+10, BM cells were isolated from irradiated $Grb10^{m/+}$ mice and $Grb10^{+/+}$ mice and stained for $SLAM^{+}KSL$ cells.

Protein Interaction assay. For detection of the binding between Grb10 and c-kit, BM KSL cells from Grb10m/+ and Grb10+/+ mice were sorted with a BD Aria sorter and treated with 100ng/ml stem cell factor (SCF) or saline for 15min at 37°C. Cells were then fixed in 4% paraformaldehyde (PFA) for 20min on a slide and incubated with anti-Grb10 (Abcam) and anti-c-kit (R&D Systems) antibodies overnight. The binding assay was performed with Duolink In

Situ Red Starter Kit (Sigma-Aldrich). Images were captured using an Axiovert 200 fluorescent microscope (Carl Zeiss, Thornwood, NY).

2.6.2 Results

Grb10 is an adaptor protein that lacks catalytic function but contains several protein binding motifs which implicate Grb10 in mediating interactions between other proteins[57]. Grb10 can bind several receptor tyrosine kinases (RTKs), including the insulin receptor, IGFR, and c-kit, and genetic studies have demonstrated that Grb10 is a negative regulator of insulin and IGF1 signaling in adipose tissue[57,115,116]. Grb10 is also a substrate for the mammalian target of rapamycin (mTOR) and Grb10 negatively regulates mTOR signaling in adipocytes[117].

Previous research suggests that in response to extracellular cytokine signals such as insulin, Grb10 was activated and shut the signaling down. However, the mechanism of Grb10 in the HSCs has not been tested. We analyzed the phosphorylation level of several signaling molecules in the Akt-mTOR pathway, as a means to detect the activation level of the signaling in the $Grb10^{m/+}$ mice compared to $Grb10^{+/+}$ mice. Interestingly, BM KSL cells from $Grb10^{m/+}$ mice showed no increase in Akt or mTOR activation in steady state (**Figure 35**). However, following 700cGy TBI, BM KSL cells from $Grb10^{m/+}$ mice displayed significantly increased mTOR activation compared to $Grb10^{+/+}$ cells (**Figure 36**). Similarly, treatment with c-kit ligand (SCF) significantly increased Akt and mTOR activation in $Grb10^{m/+}$ KSL cells compared to $Grb10^{+/+}$ KSL cells. Taken together, these data suggested that maternal deletion of Grb10 did not alter baseline Akt or mTOR activation in HSCs, but rather potentiated the responsiveness of the Akt/mTOR pathway in HSCs in the setting of stress or cytokine stimulation.

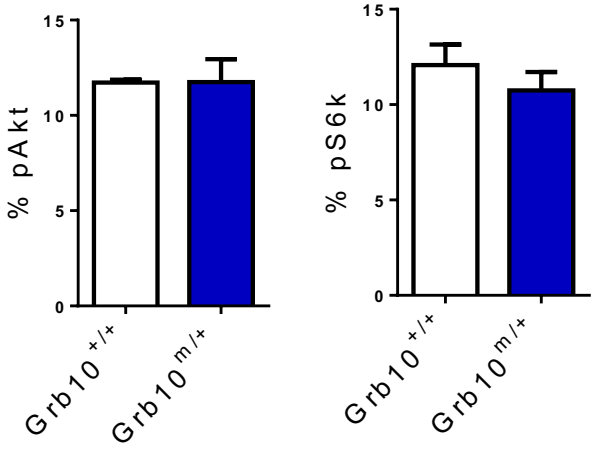

Figure 35 phosphorylation analysis of Akt and S6K in the KSL cells of Grb10$^{+/+}$ and Grb10$^{m/+}$ mice

Phosphorylation of Akt (left) and S6K (right) at steady state in Grb10$^{+/+}$ and Grb10$^{m/+}$ KSL cells (n = 5 mice / group, t-test).

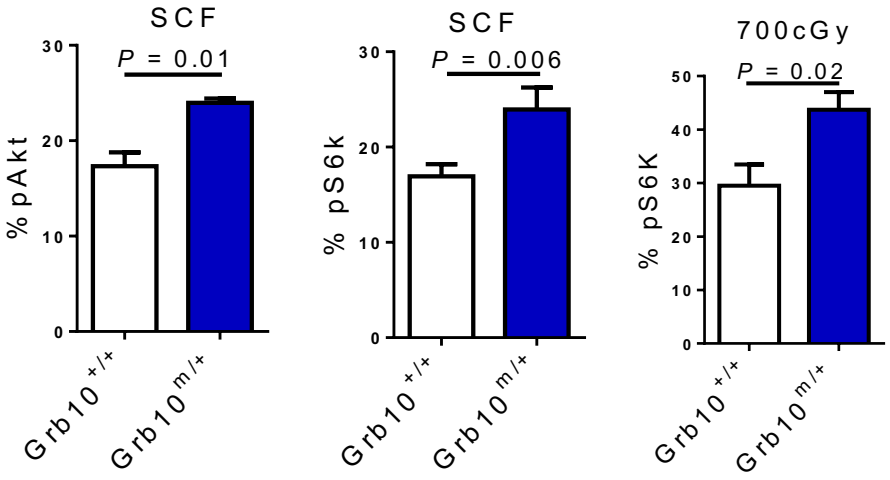

Figure 36 phosphorylation analysis of Akt and S6K in the KSL cells of Grb10$^{+/+}$ and Grb10$^{m/+}$ mice

Phosphorylation of Akt (left) (n = 4 mice / group), S6K(middle) after 5mins of SCF treatment (n = 7 mice / group) and (right) at 24h after 700cGy TBI (n = 8 mice / group), in the KSL cells of $Grb10^{+/+}$ and $Grb10^{m/+}$ mice (t-test).

Rac1 was shown to be a potential downstream molecule for mTOR signaling, although the relative regulatory relationship between Rac1 and mTOR is not clear. Of note, treatment with the mTOR antagonist, rapamycin, inhibited Rac1 activation in $Grb10^{m/+}$ lin- cells, suggesting that Rac1 activation in $Grb10^{m/+}$ HSCs was dependent, at least in part, on mTOR (**Figure 37**). Furthermore, systemic treatment of irradiated $Grb10^{m/+}$ mice with rapamycin abolished the early regeneration of the $SLAM^{+}KSL$ HSC pool which was otherwise observed in $Grb10^{m/+}$ mice compared to $Grb10^{+/+}$ mice (**Figure 38**). The regeneration of hematopoietic progenitors is also delayed in the rapamycin injected $Grb10^{m/+}$ BM cells. Previous research suggests that rapamycin has non-specific binding activity besides mTOR. To further confirm our finding, we used another mTORC1 inhibitor, CCI-779, and found that in vivo injection of CCI-779 also diminished the increased recovery of $SLAM^{+}KSL$ cells in $Grb10^{m/+}$ mice at day+10 following irradiation (**Figure 39**). In a separate study, systemic treatment of irradiated $Grb10^{m/+}$ mice with MK2206 HCI, a specific Akt inhibitor, mutated the increased regeneration of $SLAM^{+}KSL$ cells in $Grb10^{m/+}$ mice compared to $Grb10^{+/+}$ mice shortly following 550cGy irradiation. Taken all the data together, we conclude that Grb10 regulates HSC regeneration under stress conditions, at least partly through Akt-mTOR signaling pathway.

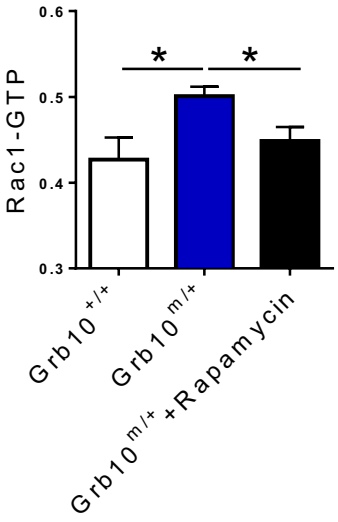

Figure 37 Rac1 overactivation assay in the lin- cells of Grb10$^{+/+}$ and Grb10$^{m/+}$ mice ± rapamycin injection

Mean levels of Rac1-GTP in BM lin$^-$ cells from *Grb10$^{m/+}$* mice and *Grb10$^{+/+}$* mice following 24-hour culture ± rapamycin (n=4/group).

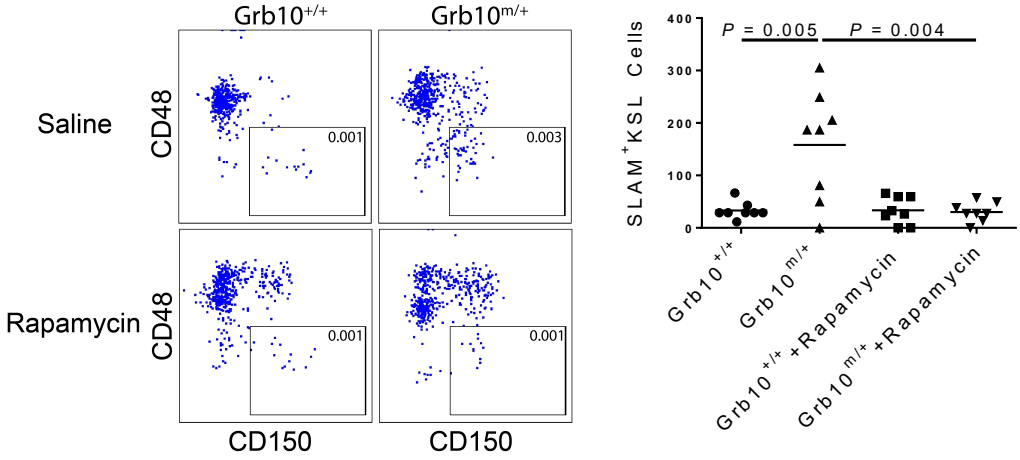

Figure 38 SLAM KSL cells analysis at day+10 after 550Gy irradiation of Grb10$^{+/+}$ and Grb10$^{m/+}$ mice ± rapamycin injection

At left, representative flow cytometric analysis of SLAM$^+$KSL cells in Grb10$^{+/+}$ mice and Grb10$^{m/+}$ mice at day +10 following 550 cGy TBI and treatment with and without rapamycin. At

right, scatter plot shows the numbers of BM SLAM^{+}KSL cells in *Grb10*$^{+/+}$ mice and *Grb10*$^{m/+}$ mice at day +10 in each group (n=8 mice/group).

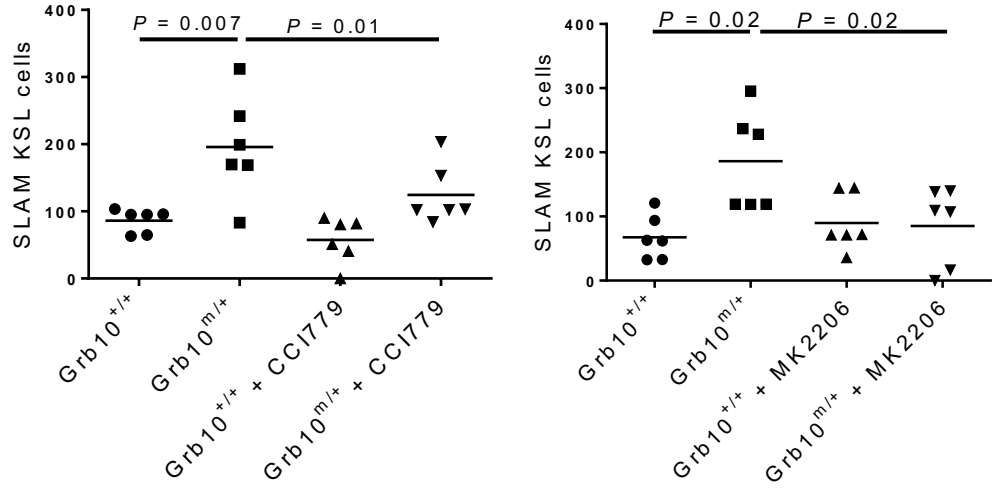

Figure 39 SLAM KSL cells analysis at day+10 after 550Gy irradiation of Grb10$^{+/+}$ and Grb10$^{m/+}$ mice ± CCI-779/MK2206 treatment

Scatter plot shows the numbers of BM SLAM^{+}KSL cells in *Grb10*$^{+/+}$ mice and *Grb10*$^{m/+}$ mice at day +10 in each group with and without CCI-779 (left) (n=6 mice/group) and MK2206 (right) (n=6 mice/group).

Previous data have suggested a functional link between Grb10 and SCF receptor c-Kit[118]. However, it has been controversial on the regulatory role of Grb10 in the signaling pathway involving receptor tyrosine kinases[119]. In our system, treatment of SCF induces overactivation of Akt-mTOR signaling in the Grb10$^{m/+}$ mice, suggesting that Grb10 negatively regulates cellular signals through c-Kit. To determine the interaction between Grb10 and c-Kit mediated signaling pathway, we performed Duolink protein binding analysis to determine the binding status of Grb10 and c-Kit. As shown in **Figure 40**, without SCF treatment, Grb10 shows no binding

activity with c-Kit. However, shortly after SCF treatment, Grb10 in $Grb10^{+/+}$ KSL cells binds to c-Kit near cell membrane. This binding activity is diminished in the $Grb10^{m/+}$ KSL cells. Treatment of $Grb10^{m/+}$ BM KSL cells with SCF enhanced the CFC increase observed in the $Grb10^{m/+}$ mice, compared to $Grb10^{+/+}$ cells treated with SCF (**Figure 41**). These data indicate that in response to extracellular signals such as SCF, Grb10 binds to cell surface receptor including c-Kit, and activate downstream signaling pathways and eventually lead to increased activity in BM stem cells.

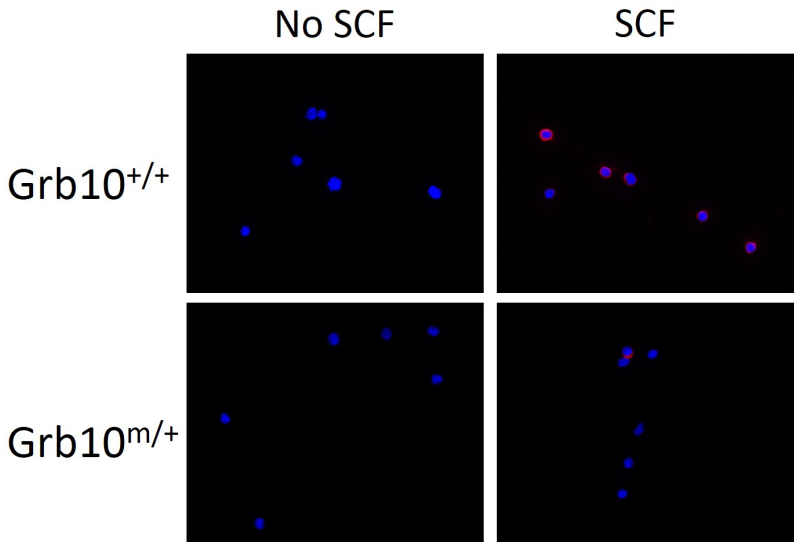

Figure 40 Binding assay of Grb10 and c-Kit

Representative fluorescence image shows the binding of Grb10 and c-kit with and without SCF treatment. Blue, DAPI; Red, Grb10-c-kit complex.

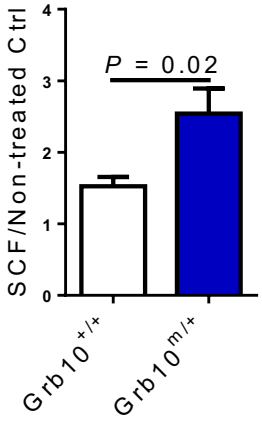

Figure 41 SCF treatment of Grb10$^{+/+}$ and Grb10$^{m/+}$ KSL cells

Mean ratios of CFC numbers with versus without SCF treatment. BM KSL cells from Grb10+/+ and Grb10m/+ mice were used to set up the assay (n = 6 / group).

2.7 Expression of Grb10 is partially regulated by transcription factor STAT5b

2.7.1 Methods

Quantitative real time PCR. RNA was isolated using the Qiagen RNeasy micro kit. RNA was reverse transcribed into cDNA using iScript cDNA synthesis kit. Using Taqman Gene Expression assays, we performed real time PCR analysis for Grb10, STAT5b, LMX1a.

siRNA. Sorted KSL cells were put into culture in the Accell Delivery Media (Dharmacon). 1nM siRNA targeting Grb10 or STAT5b were put into culture for 72h at 37°C. After 72h of treatment, cells were collected, washed with 1X DPBS, and RNAs were isolated with RNeasy Micro Kit (Qiagen).

2.7.2 Results

To determine the upstream regulation of Grb10 expression, we focused on identifying the transcription factors that have the potential to regulate Grb10 expression. Based on previous

research, deletion of the LIM homeodomain transcription factor Lmx1a in mouse embryos significantly reduces the expression of the Grb10[120]. In another research, in silico simulation discovered signal transducer and activator of transcription (STAT) 5b, to be a potential regulator for Grb10 regulation. We measured the expression of STAT5b and Lmx1a in irradiated CD34-KSL cells, where Grb10 exhibited a clear upregulation induced by irradiation (**Figure 42**). Expression of STAT5b correlates with the Grb10 expression after irradiation, although Lmx1a was not detected. To determine the functional relation between Grb10 and STAT5b, we inhibited the expression of STAT5b in sorted KSL cells, and found that inhibition of STAT5b in vitro significantly reduced the expression level of Grb10 (**Figure 43**). These data prove that regulation of Grb10 expression in response to irradiation is regulated, at least partially, by STAT5b.

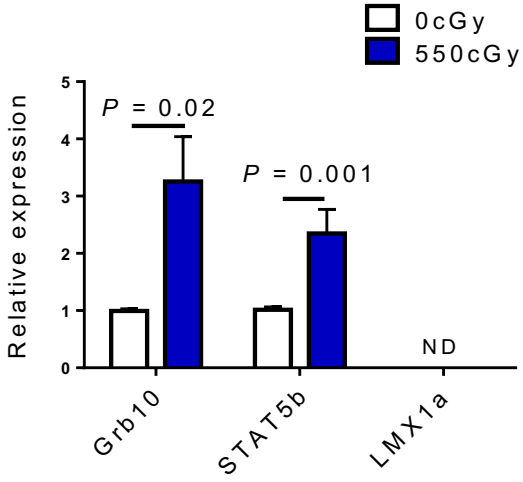

Figure 42 Expression of Grb10, STAT5b and LMX1a in CD34-KSL cells after irradiation.

Expression of Grb10, STAT5b and LMX1a in BM CD34-KSL cells at day+10 following 550cGy TBI (n = 6 / group).

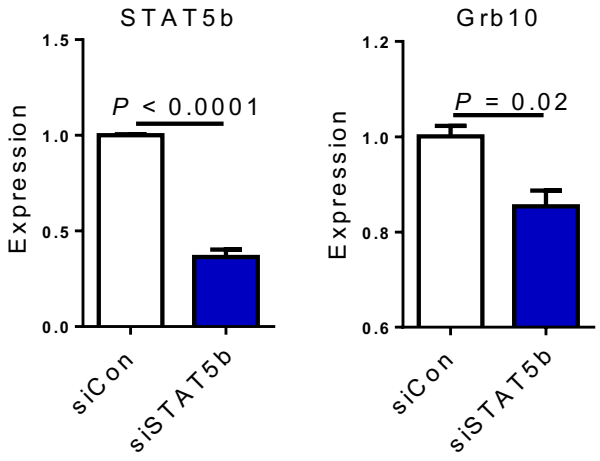

Figure 43 Expression of Grb10 in KSL cells treated with siRNA targeting STAT5b.

Expression of Grb10 (left) and STAT5b (right) in BM KSL cells at day+3 following treatment of scramble siRNA or siRNA-STAT5b (n = 6/group).

2.8 In vitro inhibition of Grb10 leads to depletion of HSCs in cytokine culture

2.8.1 Methods

Statistics. Unless stated otherwise in the Figure Legends, all graphical data are presented as means + SEM, except histograms, and significance was calculated using two-tailed Student's t test. $P < 0.05$ was considered significant. Competitive repopulating assays were compared with a two-tailed Mann-Whitney test. For all animal studies, we used a power test to determine the sample size needed for a 2-fold difference in mean with 0.8 power using a two-tailed Student's t-test. Animals in our studies were sex and age matched and littermates were used as controls.

Virus infection. shRNA sequence targeting Grb10 was purchased from Sigma-Aldrich (St. Louis). shRNA was ligated to pLL3.7 plasmid. 293FT cells were used to produce virus by co-transfecting pLL3.7 containing shRNA sequence, VSVG, and delta-8.3 (kind gift from Duke Virology Core) plasmids. At 72h after transfection, cells were centrifuged down. Supernatants

containing viral particles were enriched using an ultracentrifuge. MOI (multiplicity of infectivity) was determined by infecting 293FT cells with virus. Cells that were GFP+ (indicating virus infection) were counted at 72h after virus infection. Murine lineage$^-$c-kit$^+$sca-1$^+$ (KSL) cells were sorted with a BD FACS Aria Fusion (BD). For infection with virus, 30,000 sorted KSL cells were resuspended in 100ul X-Vivo 15 medium (Lonza), supplemented with 50 uM 2-ME (Sigma Aldrich), 10% FBS, 100ng/ml murine stem cell factor and 20ng/ml murine thrombopoietin for 24h before virus addition. MOI = 10-20 was used to infect the KSL cells.

HSC in vitro culture. Infected murine lineage$^-$c-kit$^+$sca-1$^+$ (KSL) cells were sorted with a BD FACS Aria Fusion (BD). 500 sorted KSL cells were cultured in one 96-well plate, in IMDM with 10% FBS and 1% penicillin-streptomycin supplemented with 20ng/mL thrombopoietin, 125ng/mL stem cell factor and 50ng/mL Flt-3 ligand (TSF). At day+3 and day+7 in culture, cultured cells were collected and resuspended in methylcellulose methocult M3434 (STEMCELL Technologies) and plated into a 35mm dish with grid. Cells were cultured in an incubator at 37C for 14 days and counted based on the instructions on the datasheet. Cultured cells were also stained with cell surface markers anti-c-kit APC-Cy7 (BD Biosciences), anti-Sca-1 PE (BD Biosciences), anti-lineage V450 (BD Biosciences). At day+7 in culture, 2000 cultured cells were transplanted into lethally irradiated CD45.1$^+$ B6.SJL mice via tail vein along with 2 x 10^5 host competitor BM cells. Multilineage hematopoietic cell engraftment was measured by flow cytometric analysis of the PB every 4 weeks through week 20 post-transplant, as previous described. To perform the secondary bone marrow transplantation, at 20th week following BM transplantation, 75% of the whole bone marrow cells were isolated and transplanted into lethally irradiated recipient mice. At certain times after BM transplantation, PB was analyzed by flow cytometry.

2.8.2 Results

To determine the therapeutic effect of Grb10 modulation, we generated a lentivirus expressing shRNA targeting Grb10 and used it to infect purified KSL cells and put the infected cells in culture. At day+3 in culture, Grb10 expression was knocked down by 50% in the shRNA-Grb10 infected cells. Colony-forming cells and KSL cells are significantly decreased in the Grb10-deficient cells compared to wild-type cells at day+7 in culture. To our surprise, recipient mice transplanted with Grb10-deficient donor cells show significantly decreased multi-lineage donor engraftment compared to mice transplanted with wild-type cells (**Figure 44**). To evaluate the effect of Grb10 deficiency on the long-term HSCs, we isolated bone marrows from primary recipient mice, and performed secondary transplantation by transplanting the primary bone marrow cells into lethally irradiated mice together with a competitor dose. Peripheral blood analysis at 12^{th} week after secondary transplantation indicates a significant decrease in donor engraftment in the mice transplanted with Grb10 deficient cells compared to wild-type control. Data from bone marrow analysis of both primary and secondary recipient mice confirmed a 10-fold decrease in the donor engraftment caused by Grb10 deficiency in the donor cells, compared to wild-type counterparts. These data suggest that virus-mediated Grb10 deficiency leads to HSC depletion in vitro. The different Grb10 deficiency phenotype in vivo and in vitro may indicate the necessity of the precise modulation of Grb10 expression level.

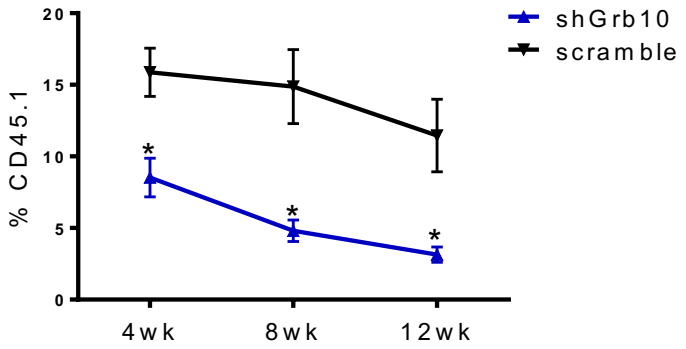

Figure 44 Time course of bone marrow transplantation assay with virus-infected KSL cells.

Donor (CD45.1+) cell engraftment over time in the PB of recipient CD45.2+ mice transplanted with 2000 KSL cells infected with either scramble virus or shGrb10-expressing virus, together with $2x10^5$ CD45.2+ competitor BM cells (n = 10/group, P=0.04, P=0.002, and P=0.004 for 4, 8, 12 weeks, respectively, Mann-Whitney).

Chapter 3 Discussion and future experiments

3.1 Discussion

Recently studies have identified several different signals from stem cell niche, including notch[121,122], TGF-beta[123], and cytokines such as EGF[30] and pleiotrophin[39] can regulate HSC regeneration following injury. However, the intrinsic mechanisms through which HSC regenerate remain poorly understood. Here we show that Grb10, an adaptor protein involved in receptor tyrosine kinase signaling pathway, was significantly upregulated by irradiation. Genetic deletion of Grb10 promotes HSC engraftment capability, while Grb10 ablation accelerates HSC regeneration following irradiation. Grb10 belongs to the Grb family of proteins including Grb7 and Grb14[46]. Members in this family contain a highly conserved SH2 domain. This SH2 domain has been proven to be important for binding to phosphor-tyrosines of growth factor receptors and intracellular signaling proteins. Grb10 binds to cell surface receptors including c-kit, EGFR and

Ret, the signaling pathways through which are critical for hematopoietic stem cell self-renewal or regeneration[29,30,124]. Taken all these previous data together, Grb10 has the potential to be a "central regulator" for HSC function. Commensurate with this, our data show for the first time that Grb10 regulates both HSC self-renewal and regeneration.

Genomic imprinting, in which imprinted genes are expressed from only one parental allele, has long been found to be critical for pre- and post-natal growth, as well as brain function and behavior[65,125]. Of the imprinted genes, a subset named imprinted gene network (IGN), were highly expressed in long-term HSCs compared to hematopoietic progenitors or mature blood cells[69]. IGN expression was downregulated in multiple tissues during postnatal growth, suggesting a relationship between the IGN and "stemness"[68]. Among the members of the IGN, cdkn1c, or p57, was found to maintain HSC quiescence in a cooperative manner with p27, while ablation of necdin, a cell cycle regulator of neuronal cells, promotes recovery of hematopoietic cells following irradiation injury[126,127]. However, the role of genomic imprinting has not been discussed in these two researches. Recently, a group revealed that the maternal imprinting at H19-Igf2 regulates HSCs proliferation through the activation of Igf2-Igfr1 signaling pathway[70]. The same group identified another maternally imprinted locus, Dlk1-Gtl2, to be involved in LT-HSC preservation by modulation of PI3K-mTOR signaling[71]. Here, we showed that Grb10, another maternally imprinted gene, is a key regulator for HSC self-renewal and regeneration. Taken together, these data provide the first evidence that gene imprinting is closely associated with hematopoietic stem cell regulation.

Mechanistically, we have demonstrated that Grb10-deficient hematopoietic stem/progenitor cells (HSPCs) possess enhanced proliferative potential in vivo following transplantation or radiation injury, coupled with augmented migratory capacity. We show further that the accentuated

proliferative capacity and migratory potential of Grb10- deficient HSPCs is dependent on Rac activation. We hypothesize that maternal deletion of Grb10 promotes Rac1 activation via intermediate effects on mTOR signaling. mTOR has been shown to promote mammary epithelial cell motility and survival via Rac1 activation[128] and Rac1-mediated activation and aggregation of platelets has been shown to be under the control of mTOR[129]. We found that mTOR inhibition with rapamycin blunted Rac1 activation in Grb10-deficient BM cells and abrogated the accelerated recovery of the HSC pool following TBI in $Grb10^{m/+}$ mice. Interestingly, Grb10-deficient HSPCs did not display increased activation of mTOR in steady state, but mTOR activation was increased in response to SCF treatment or stress (irradiation). We propose that Grb10 deletion augments the capacity of HSCs to respond to stress or injury via potentiation of mTOR/Rac1 signaling. In that regard, our findings are consistent with the recent observation that mTOR signaling is necessary and sufficient for muscle stem cell regeneration via transition from G_0 to G_{Alert} cell cycle state[130]. Of note, since Grb10 deletion did not cause constitutive activation of the mTOR pathway in HSCs, we did not observe exhaustion of the HSC pool as has been described following deletion of the mTOR inhibitors, phosphatase and tensin homologue (PTEN) and the Tuberous Sclerosis Complex 1 (TSC1)[103,131,132]. Rather, Grb10 deletion substantially increased the regeneration of long-term repopulating HSCs in irradiated mice, suggesting a previously unrecognized role for the Grb10/mTOR/Rac1 pathway in regulating HSC regeneration.

Rac subfamily of Rho guanosine triphosphatases (GTPases) have been proven to have critical regulatory role in hematopoiesis[72]. Within the Rac family, Rac2 ablation causes the abnormal interaction of HSCs with the hematopoietic microenvironment, while Rac1 deficiency leads to a decrease in the short-term engraftment of HSCs[74]. Recent studies show that Rac1 and Rac2

double deficiency induces a significant decrease in the transendothelial migration capability of progenitor cells[112]. Our lab previously showed that PTPS, a receptor protein tyrosine phosphatase, regulates the repopulating capacity of HSCs through Rac1 activation, confirming the key regulatory role of Rac1 in HSCs[23]. Here, we discovered that Grb10 maternal deletion overactivated Rac1, and that Grb10 deficient bone marrow cells have increased transendothelial migration capability, while treatment of EHT1864, a Rac inhibitor, abrogated the effect. Our data coincide with the central regulatory role of Rac1 in the HSC mobilization. Although no directly evidence shows a direct binding of Grb10 to Rac1, in *C. elegans*, Mig-10, a protein that is structurally similar to Grb family protein, binds to Rac1[133]. Whether Grb10 regulates Rac1 directly or through certain signaling pathways remains to be an interesting question. In addition to this, we will also perform experiments to determine whether other Rac proteins such as Rac2 or Rac3 are involved in the Grb10 signaling pathway.

Recent studies have established Grb10 as a negative regulator of Akt-mTOR signaling pathway[134,135]. Activated mTORC1 phosphorylates and stabilizes Grb10 protein, then Grb10 binds to cell surface receptors or insulin receptor substrate-1 (IRS1) in a competitive manner, tuning down the signaling[135]. mTOR has a well-established role in the regulation of protein and lipid synthesis, lysosome biogenesis and energy metabolism[85]. Researches from several groups show that deletion of different signaling molecules in Akt-mTOR pathway, including *PTEN* and *TSC1*, depletes HSCs as indicated by competitive transplantation assay[43,89,105]. However, the function of mTOR signaling during irradiation has not been clearly examined. We showed that Grb10 ablation leads to overactivation of mTOR signaling following irradiation. Injection of rapamycin, a mTORC1 inhibitor, abrogated the accelerated recovery of SLAM KSL cells in $Grb10^{m/+}$ mice following irradiation. In a separate study, we injected rapamycin into the

recipient mice transplanted with *Grb10*$^{+/+}$ and *Grb10*$^{m/+}$ whole bone marrow cells (data not shown). The injection of rapamycin did not influence the increased donor engraftment of the *Grb10*$^{m/+}$ BM cells compared to *Grb10*$^{+/+}$ cells. These data indicate that under non-irradiation settings, Grb10 does not regulate HSCs through mTOR. One possible reason is the existence of other negative feedback loops, especially the one via activation of S6K, compensates for the Grb10 ablation. Activated S6k phosphorylates IRS1 and leads to its degradation[85]. On the contrary, no previous report has shown regulatory molecules similar to *PTEN* or *TSC1*. However, irradiation may induce a more dramatic influence in the signaling that is over the limit of the compensation mechanism. In accordance with our data, in the neuronal system, activation of mTOR signaling promotes the regeneration of axon following injury, confirming a beneficial role of mTOR signaling during organ regeneration[136-138]. Our data reveal a novel regulator and irradiation mitigator of HSCs named Grb10, and suggest that pharmacological inhibition of Grb10 has therapeutic benefit in the bone marrow transplantation and hematological regeneration following irradiation injury.

3.2 Future directions

Grb10 ablation promotes HSC regeneration for more than 10-folds. That provides scientific bases to target Grb10 for potential therapeutic methods. Grb10 is an adaptor protein, which increases the difficulty to target this protein in the drug development. Utilizing bioinformatics tools, I will propose these experiments to find a drug target.

3.2.1 RNA-seq of Grb10 knockout mice

Grb10 is an intracellular protein, which limits the way we can apply to inhibit the expression of Grb10. To find a drug target, we will isolate BM c-kit^{+}sca-1^{+} lineage^{-} cells from Grb10$^{+/+}$ and Grb10$^{m/+}$ mice, which enriches BM HSCs, extract mRNA and perform RNA-seq comparing the

mRNA profile between $Grb10^{+/+}$ and $Grb10^{m/+}$ mice. We will perform gene ontology analysis to identify genes that are cellular surface receptors. We aim to find certain cell surface receptor that is up-regulated or down-regulated in the $Grb10^{m/+}$ mice compared to $Grb10^{+/+}$ mice. Then we will test the agonist or antagonist of this receptor on HSCs.

To perform the pathway discovery analysis, we will irradiate $Grb10^{+/+}$ and $Grb10^{m/+}$ mice. At different time points after irradiation, we will collect BM KSL cells and run RNA-seq or microarray analysis. Then we will perform pathway discovery analysis using the same principle as in the phylogenetic profiling analyses that the genes in the same pathway tend to co-function under different conditions. Once we identify the genes that are related to Grb10 signaling pathway, we can then develop inhibitors for the genes in the Grb10 signaling pathway.

3.2.2 Immunoprecipitation of Grb10

Previous research suggests that Grb10 binds to cell surface receptors, specifically receptor tyrosine kinases. In another effect to identify signals that are regulated by Grb10, we will perform immunoprecipitation of Grb10. Then we will perform tandem mass spectrometry on the proteins that are pulled down by Grb10. Then we will map the results to the protein database to find the receptor proteins that interact with Grb10.

3.2.3 Drug interaction screen

To screen drugs that inhibit Grb10 function, we will utilize the principle of defining drug-gene interactions. Our data suggests that Grb10 knock out promotes the proliferation of HSCs. We will use cell growth as the readout. In this situation, we will normalize the growth rate for a knockout versus WT condition. Then we will screen a library of drugs and normalize the growth rate for a drug (with drug vs. without drug). Then we will measure the combined effect by treating the Grb10 knock out cells with drug. By comparing the combined effect and the

individual effect of Grb10 knock out and drug treatment, we can screen for drugs that have interaction with Grb10.

3.2.4 Other molecules that are upregulated by irradiation

Methods

HSC in vitro culture. Murine lineage$^-$c-kit$^+$sca1$^+$ (KSL) cells were sorted with a BD FACS Aria Fusion (BD). 500 sorted KSL cells were cultured in one 96-well plate, in IMDM with 10% FBS and 1% penicillin-streptomycin supplemented with 20ng/mL thrombopoietin, 125ng/mL stem cell factor and 50ng/mL Flt-3 ligand (TSF). Purified recombinant protein osteocalcin (Bachem) and osteonectin (R&D systems) were put into the culture in a range of 0.3ng/ml to 1000ng/ml, and 0.1ug/ml to 5ug/ml, respectively. At day+7 in culture, cells were collected and counted with an automated cell counter (Bio-rad). Cells were stained with cell surface markers anti-c-kit APC-Cy7 (BD Biosciences), anti-Sca-1 PE (BD Biosciences), anti-lineage V450 (BD Biosciences).

Results

To look at other molecules that are shown to have altered expression induced by irradiation, we focus on osteocalcin (OCN) and osteonectin (ON), both of which show specific increased expression after irradiation. Osteocalcin is one of the few proteins that have restricted expression in osteoblasts and has long been used as a marker for osteoblast staining. Recently, whole-organism approaches have started to reveal novel functions of osteocalcin on the physiology of the body. Osteocalcin secreted from in vitro cultured osteoblast promotes the production of testosterone by the testes, while it has no influence on the ovary-derived estrogen[139]. In a separate study, mice that lack osteocalcin expression show decreased beta-cell proliferation, glucose intolerance and insulin resistance[140]. These data suggest the possibility that osteocalcin can act as a signaling molecule on other organs including bone marrow. Osteonectin is also

abundant in bone and has been shown to be related to angiogenesis, metalloproteinase expression, cell proliferation and cell-matrix interactions[141]. The expression of osteonectin correlates with tumor progression[142].

The expression of both osteocalcin and osteonectin is upregated at 550cGy in KSL cells in vitro, although the kinetics of upregulation is different. Triggered by irradiation, OCN is rapidly upregulated in the KSL cells at 12h following irradiation, while the response of osteonectin to irradiation occurs at 24h following irradiation (**Figure 45**). For both of the genes, the upregulation is only observed in KSL cells which enrich for HSCs, but not in c-kit^{+}sca1^{-}lin^{-} progenitor cells, indicating a stem cell specific function. To determine whether OCN or ON have the potential to be a growth factor for HSCs, we performed 7-day culture of KSL cells with a range of different dosages of OCN and ON. Treatment of 1ug/ml ON in KSL cells shows a potential trend of KSL increase, while a OCN dose as low as 0.3ng/ml is sufficient to promote the proliferation of KSL cells in vitro (**Figure 46**). These preliminary data suggest that OCN and ON have the potential to be growth factors for HSC expansion.

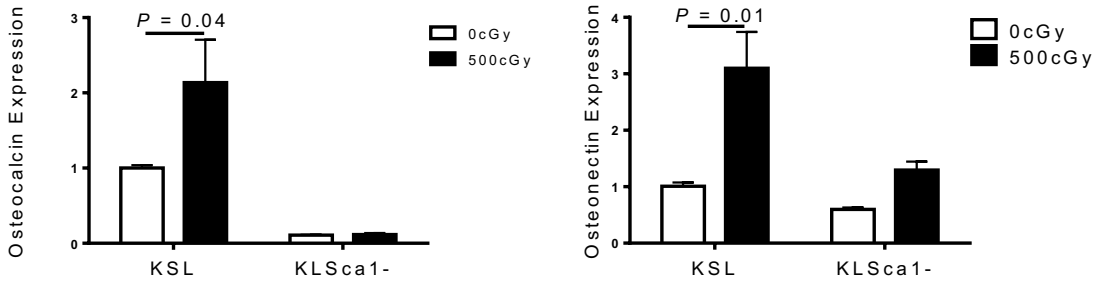

Figure 45 Osteocalcin and osteonectin expression in KSL and KLSca1- cells after 550cGy irradiation

Expression of osteocalcin and osteonectin in KSL and KLSca1- cells at 12 (left) (n = 4/group) and 24 (right) (n = 4/group) hours after 550cGy irradiation.

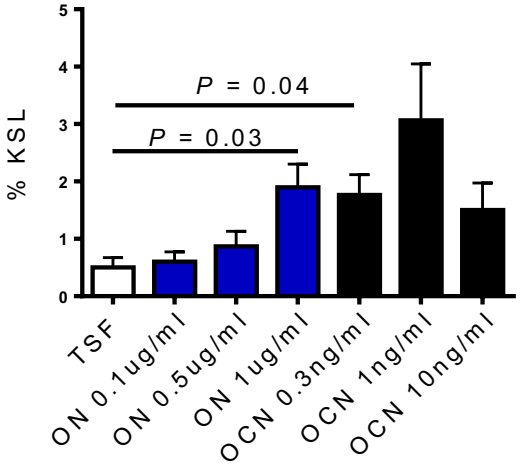

Figure 46 In vitro culture of BM KSL cells with osteocalcin and osteonectin

Mean percentage of BM KSL cells at day+7 after in vitro culture with TSF medium + Osteocalcin or osteonectin (n=6 /group, t-test).

References

1. Orkin, S.H. & Zon, L.I. Hematopoiesis: an evolving paradigm for stem cell biology. *Cell* **132**, 631-644 (2008).
2. Choi, K., Kennedy, M., Kazarov, A., Papadimitriou, J.C. & Keller, G. A common precursor for hematopoietic and endothelial cells. *Development* **125**, 725-732 (1998).
3. Ueno, H. & Weissman, I.L. Clonal analysis of mouse development reveals a polyclonal origin for yolk sac blood islands. *Dev Cell* **11**, 519-533 (2006).
4. McGrath, K.E., Koniski, A.D., Maltby, K.M., McGann, J.K. & Palis, J. Embryonic Expression and Function of the Chemokine SDF-1 and Its Receptor, CXCR4. *Developmental Biology* **213**, 442-456 (1999).
5. Matsui, Y., Zsebo, K.M. & Hogan, B.L.M. Embryonic expression of a haematopoietic growth factor encoded by the SI locus and the ligand for c-kit. *Nature* **347**, 667-669 (1990).
6. Ema, H.*, et al.* Adult mouse hematopoietic stem cells: purification and single-cell assays. *Nat Protoc* **1**, 2979-2987 (2006).
7. Wang, J.C., Doedens, M. & Dick, J.E. Primitive human hematopoietic cells are enriched in cord blood compared with adult bone marrow or mobilized peripheral blood as measured by the quantitative in vivo SCID-repopulating cell assay. *Blood* **89**, 3919-3924 (1997).
8. Weissman, I.L. Stem cells: units of development, units of regeneration, and units in evolution. *Cell* **100**, 157-168 (2000).

9. Akashi, K., Traver, D., Miyamoto, T. & Weissman, I.L. A clonogenic common myeloid progenitor that gives rise to all myeloid lineages. *Nature* **404**, 193-197 (2000).

10. Kondo, M., Weissman, I.L. & Akashi, K. Identification of clonogenic common lymphoid progenitors in mouse bone marrow. *Cell* **91**, 661-672 (1997).

11. Manz, M.G., Traver, D., Miyamoto, T., Weissman, I.L. & Akashi, K. Dendritic cell potentials of early lymphoid and myeloid progenitors. *Blood* **97**, 3333-3341 (2001).

12. Traver, D.*, et al.* Development of CD8alpha-positive dendritic cells from a common myeloid progenitor. *Science* **290**, 2152-2154 (2000).

13. Petrie, H.T. & Kincade, P.W. Many roads, one destination for T cell progenitors. *J Exp Med* **202**, 11-13 (2005).

14. Lai, A.Y. & Kondo, M. Identification of a bone marrow precursor of the earliest thymocytes in adult mouse. *Proc Natl Acad Sci U S A* **104**, 6311-6316 (2007).

15. Okada, S.*, et al.* In vivo and in vitro stem cell function of c-kit- and Sca-1-positive murine hematopoietic cells. *Blood* **80**, 3044-3050 (1992).

16. Yang, L.*, et al.* Identification of Lin(-)Sca1(+)kit(+)CD34(+)Flt3- short-term hematopoietic stem cells capable of rapidly reconstituting and rescuing myeloablated transplant recipients. *Blood* **105**, 2717-2723 (2005).

17. Kiel, M.J.*, et al.* SLAM family receptors distinguish hematopoietic stem and progenitor cells and reveal endothelial niches for stem cells. *Cell* **121**, 1109-1121 (2005).

18. Ding, L. & Morrison, S.J. Haematopoietic stem cells and early lymphoid progenitors occupy distinct bone marrow niches. *Nature* **495**, 231-235 (2013).

19. Notta, F.*, et al.* Isolation of single human hematopoietic stem cells capable of long-term multilineage engraftment. *Science* **333**, 218-221 (2011).

20. Mayani, H., Dragowska, W. & Lansdorp, P.M. Characterization of functionally distinct subpopulations of CD34+ cord blood cells in serum-free long-term cultures supplemented with hematopoietic cytokines. *Blood* **82**, 2664-2672 (1993).

21. Baum, C.M., Weissman, I.L., Tsukamoto, A.S., Buckle, A.M. & Peault, B. Isolation of a candidate human hematopoietic stem-cell population. *Proc Natl Acad Sci U S A* **89**, 2804-2808 (1992).

22. Hao, Q.L., Shah, A.J., Thiemann, F.T., Smogorzewska, E.M. & Crooks, G.M. A functional comparison of CD34 + CD38- cells in cord blood and bone marrow. *Blood* **86**, 3745-3753 (1995).

23. Quarmyne, M.*, et al.* Protein tyrosine phosphatase-sigma regulates hematopoietic stem cell-repopulating capacity. *J Clin Invest* **125**, 177-182 (2015).

24. Wognum, B., Yuan, N., Lai, B. & Miller, C.L. Colony forming cell assays for human hematopoietic progenitor cells. *Methods Mol Biol* **946**, 267-283 (2013).

25. Liu, M., Miller, C.L. & Eaves, C.J. Human long-term culture initiating cell assay. *Methods Mol Biol* **946**, 241-256 (2013).

26. Morrison, S.J. & Scadden, D.T. The bone marrow niche for haematopoietic stem cells. *Nature* **505**, 327-334 (2014).

27. Zhang, J.*, et al.* Identification of the haematopoietic stem cell niche and control of the niche size. *Nature* **425**, 836-841 (2003).

28. Greenbaum, A.*, et al.* CXCL12 in early mesenchymal progenitors is required for haematopoietic stem-cell maintenance. *Nature* **495**, 227-230 (2013).

29. Ding, L., Saunders, T.L., Enikolopov, G. & Morrison, S.J. Endothelial and perivascular cells maintain haematopoietic stem cells. *Nature* **481**, 457-462 (2012).

30. Doan, P.L.*, et al.* Epidermal growth factor regulates hematopoietic regeneration after radiation injury. *Nat Med* **19**, 295-304 (2013).

31. Himburg, H.A.*, et al.* Pleiotrophin regulates the retention and self-renewal of hematopoietic stem cells in the bone marrow vascular niche. *Cell Rep* **2**, 964-975 (2012).

32. Kennedy, M.*, et al.* A common precursor for primitive erythropoiesis and definitive haematopoiesis. *Nature* **386**, 488-493 (1997).

33. Sacchetti, B.*, et al.* Self-renewing osteoprogenitors in bone marrow sinusoids can organize a hematopoietic microenvironment. *Cell* **131**, 324-336 (2007).

34. Pinho, S.*, et al.* PDGFRalpha and CD51 mark human nestin+ sphere-forming mesenchymal stem cells capable of hematopoietic progenitor cell expansion. *J Exp Med* **210**, 1351-1367 (2013).

35. Yamazaki, S.*, et al.* Nonmyelinating Schwann cells maintain hematopoietic stem cell hibernation in the bone marrow niche. *Cell* **147**, 1146-1158 (2011).

36. Mettler, F.A., Jr. & Voelz, G.L. Major radiation exposure--what to expect and how to respond. *N Engl J Med* **346**, 1554-1561 (2002).

37. Testa, N.G., Hendry, J.H. & Molineux, G. Long-term bone marrow damage in experimental systems and in patients after radiation or chemotherapy. *Anticancer Res* **5**, 101-110 (1985).

38. Mauch, P.*, et al.* Hematopoietic stem cell compartment: acute and late effects of radiation therapy and chemotherapy. *Int J Radiat Oncol Biol Phys* **31**, 1319-1339 (1995).

39. Himburg, H.A.*, et al.* Pleiotrophin regulates the expansion and regeneration of hematopoietic stem cells. *Nat Med* **16**, 475-482 (2010).

40. Himburg, H.A.*, et al.* Pleiotrophin mediates hematopoietic regeneration via activation of RAS. *J Clin Invest* **124**, 4753-4758 (2014).

41. Iwanaga, H.*, et al.* Ruptured cerebral aneurysms missed by initial angiographic study. *Neurosurgery* **27**, 45-51 (1990).

42. Muramoto, G.G.*, et al.* Inhibition of aldehyde dehydrogenase expands hematopoietic stem cells with radioprotective capacity. *Stem Cells* **28**, 523-534 (2010).

43. Kobayashi, H.*, et al.* Angiocrine factors from Akt-activated endothelial cells balance self-renewal and differentiation of haematopoietic stem cells. *Nat Cell Biol* **12**, 1046-1056 (2010).

44. Lichtman, M.A. Battling the hematological malignancies: the 200 years' war. *Oncologist* **13**, 126-138 (2008).

45. Chabner, B.A. & Roberts, T.G., Jr. Timeline: Chemotherapy and the war on cancer. *Nat Rev Cancer* **5**, 65-72 (2005).

46. Holt, L.J. & Siddle, K. Grb10 and Grb14: enigmatic regulators of insulin action--and more? *Biochem J* **388**, 393-406 (2005).

47. Ooi, J.*, et al.* The cloning of Grb10 reveals a new family of SH2 domain proteins. *Oncogene* **10**, 1621-1630 (1995).

48. Margolis, B. The GRB family of SH2 domain proteins. *Prog Biophys Mol Biol* **62**, 223-244 (1994).

49. He, W., Rose, D.W., Olefsky, J.M. & Gustafson, T.A. Grb10 interacts differentially with the insulin receptor, insulin-like growth factor I receptor, and epidermal growth factor receptor via the Grb10 Src homology 2 (SH2) domain and a second novel domain located between the pleckstrin homology and SH2 domains. *J Biol Chem* **273**, 6860-6867 (1998).

50. Laviola, L.*, et al.* The adapter protein Grb10 associates preferentially with the insulin receptor as compared with the IGF-I receptor in mouse fibroblasts. *J Clin Invest* **99**, 830-837 (1997).

51. Gruppuso, P.A., Boylan, J.M. & Vaslet, C.A. Identification of candidate growth-regulating genes that are overexpressed in late gestation fetal liver in the rat. *Biochim Biophys Acta* **1494**, 242-247 (2000).

52. Kasus-Jacobi, A.*, et al.* Identification of the rat adapter Grb14 as an inhibitor of insulin actions. *J Biol Chem* **273**, 26026-26035 (1998).

53. Margolis, B.*, et al.* High-efficiency expression/cloning of epidermal growth factor-receptor-binding proteins with Src homology 2 domains. *Proc Natl Acad Sci U S A* **89**, 8894-8898 (1992).

54. Frantz, J.D., Giorgetti-Peraldi, S., Ottinger, E.A. & Shoelson, S.E. Human GRB-IRbeta/GRB10. Splice variants of an insulin and growth factor receptor-binding protein with PH and SH2 domains. *J Biol Chem* **272**, 2659-2667 (1997).

55. Daly, R.J., Sanderson, G.M., Janes, P.W. & Sutherland, R.L. Cloning and characterization of GRB14, a novel member of the GRB7 gene family. *J Biol Chem* **271**, 12502-12510 (1996).

56. Wang, J.*, et al.* Grb10, a positive, stimulatory signaling adapter in platelet-derived growth factor BB-, insulin-like growth factor I-, and insulin-mediated mitogenesis. *Mol Cell Biol* **19**, 6217-6228 (1999).

57. Charalambous, M.*, et al.* Disruption of the imprinted Grb10 gene leads to disproportionate overgrowth by an Igf2-independent mechanism. *Proc Natl Acad Sci U S A* **100**, 8292-8297 (2003).

58. Cooney, G.J.*, et al.* Improved glucose homeostasis and enhanced insulin signalling in Grb14-deficient mice. *EMBO J* **23**, 582-593 (2004).

59. Mounier, C.*, et al.* Specific inhibition by hGRB10zeta of insulin-induced glycogen synthase activation: evidence for a novel signaling pathway. *Mol Cell Endocrinol* **173**, 15-27 (2001).

60. Wick, K.R.*, et al.* Grb10 inhibits insulin-stimulated insulin receptor substrate (IRS)-phosphatidylinositol 3-kinase/Akt signaling pathway by disrupting the association of IRS-1/IRS-2 with the insulin receptor. *J Biol Chem* **278**, 8460-8467 (2003).

61. Morrione, A.*, et al.* mGrb10 interacts with Nedd4. *J Biol Chem* **274**, 24094-24099 (1999).

62. Vecchione, A., Marchese, A., Henry, P., Rotin, D. & Morrione, A. The Grb10/Nedd4 complex regulates ligand-induced ubiquitination and stability of the insulin-like growth factor I receptor. *Mol Cell Biol* **23**, 3363-3372 (2003).

63. Nantel, A., Mohammad-Ali, K., Sherk, J., Posner, B.I. & Thomas, D.Y. Interaction of the Grb10 adapter protein with the Raf1 and MEK1 kinases. *J Biol Chem* **273**, 10475-10484 (1998).

64. Han, D.C., Shen, T.L. & Guan, J.L. Role of Grb7 targeting to focal contacts and its phosphorylation by focal adhesion kinase in regulation of cell migration. *J Biol Chem* **275**, 28911-28917 (2000).

65. Wood, A.J. & Oakey, R.J. Genomic imprinting in mammals: emerging themes and established theories. *PLoS Genet* **2**, e147 (2006).

66. Morison, I.M., Paton, C.J. & Cleverley, S.D. The imprinted gene and parent-of-origin effect database. *Nucleic Acids Res* **29**, 275-276 (2001).

67. Moore, T. & Haig, D. Genomic imprinting in mammalian development: a parental tug-of-war. *Trends Genet* **7**, 45-49 (1991).

68. Lui, J.C., Finkielstain, G.P., Barnes, K.M. & Baron, J. An imprinted gene network that controls mammalian somatic growth is down-regulated during postnatal growth deceleration in multiple organs. *Am J Physiol Regul Integr Comp Physiol* **295**, R189-196 (2008).

69. Berg, J.S.*, et al.* Imprinted genes that regulate early mammalian growth are coexpressed in somatic stem cells. *PLoS One* **6**, e26410 (2011).

70. Venkatraman, A.*, et al.* Maternal imprinting at the H19-Igf2 locus maintains adult haematopoietic stem cell quiescence. *Nature* **500**, 345-349 (2013).

71. Qian, P.*, et al.* The Dlk1-Gtl2 Locus Preserves LT-HSC Function by Inhibiting the PI3K-mTOR Pathway to Restrict Mitochondrial Metabolism. *Cell Stem Cell* **18**, 214-228 (2016).

72. Williams, D.A., Zheng, Y. & Cancelas, J.A. Rho GTPases and regulation of hematopoietic stem cell localization. *Methods Enzymol* **439**, 365-393 (2008).

73. Gu, Y.*, et al.* RhoH GTPase recruits and activates Zap70 required for T cell receptor signaling and thymocyte development. *Nat Immunol* **7**, 1182-1190 (2006).

74. Gu, Y.*, et al.* Hematopoietic cell regulation by Rac1 and Rac2 guanosine triphosphatases. *Science* **302**, 445-449 (2003).

75. Cancelas, J.A., Jansen, M. & Williams, D.A. The role of chemokine activation of Rac GTPases in hematopoietic stem cell marrow homing, retention, and peripheral mobilization. *Exp Hematol* **34**, 976-985 (2006).

76. Corbetta, S.*, et al.* Generation and characterization of Rac3 knockout mice. *Mol Cell Biol* **25**, 5763-5776 (2005).

77. Bolis, A., Corbetta, S., Cioce, A. & de Curtis, I. Differential distribution of Rac1 and Rac3 GTPases in the developing mouse brain: implications for a role of Rac3 in Purkinje cell differentiation. *Eur J Neurosci* **18**, 2417-2424 (2003).

78. Tao, W.*, et al.* The TRQQKRP motif located near the C-terminus of Rac2 is essential for Rac2 biologic functions and intracellular localization. *Blood* **100**, 1679-1688 (2002).

79. Ridley, A.J. & Hall, A. The small GTP-binding protein rho regulates the assembly of focal adhesions and actin stress fibers in response to growth factors. *Cell* **70**, 389-399 (1992).

80. del Pozo, M.A., Vicente-Manzanares, M., Tejedor, R., Serrador, J.M. & Sanchez-Madrid, F. Rho GTPases control migration and polarization of adhesion molecules and cytoskeletal ERM components in T lymphocytes. *Eur J Immunol* **29**, 3609-3620 (1999).

81. Szczur, K., Xu, H., Atkinson, S., Zheng, Y. & Filippi, M.D. Rho GTPase CDC42 regulates directionality and random movement via distinct MAPK pathways in neutrophils. *Blood* **108**, 4205-4213 (2006).

82. Yang, L.*, et al.* Cdc42 critically regulates the balance between myelopoiesis and erythropoiesis. *Blood* **110**, 3853-3861 (2007).

83. Welsh, C.F.*, et al.* Timing of cyclin D1 expression within G1 phase is controlled by Rho. *Nat Cell Biol* **3**, 950-957 (2001).

84. Sordella, R., Jiang, W., Chen, G.C., Curto, M. & Settleman, J. Modulation of Rho GTPase signaling regulates a switch between adipogenesis and myogenesis. *Cell* **113**, 147-158 (2003).

85. Laplante, M. & Sabatini, D.M. mTOR signaling in growth control and disease. *Cell* **149**, 274-293 (2012).

86. Peterson, T.R.*, et al.* DEPTOR is an mTOR inhibitor frequently overexpressed in multiple myeloma cells and required for their survival. *Cell* **137**, 873-886 (2009).

87. Jacinto, E.*, et al.* Mammalian TOR complex 2 controls the actin cytoskeleton and is rapamycin insensitive. *Nat Cell Biol* **6**, 1122-1128 (2004).

88. Cadet, J.*, et al.* Assessment of oxidative base damage to isolated and cellular DNA by HPLC-MS/MS measurement. *Free Radic Biol Med* **33**, 441-449 (2002).

89. Inoki, K.*, et al.* TSC2 integrates Wnt and energy signals via a coordinated phosphorylation by AMPK and GSK3 to regulate cell growth. *Cell* **126**, 955-968 (2006).

90. Lee, D.F.*, et al.* IKK beta suppression of TSC1 links inflammation and tumor angiogenesis via the mTOR pathway. *Cell* **130**, 440-455 (2007).

91. Inoki, K., Zhu, T. & Guan, K.L. TSC2 mediates cellular energy response to control cell growth and survival. *Cell* **115**, 577-590 (2003).

92. Ma, X.M. & Blenis, J. Molecular mechanisms of mTOR-mediated translational control. *Nat Rev Mol Cell Biol* **10**, 307-318 (2009).

93. Mayer, C., Zhao, J., Yuan, X. & Grummt, I. mTOR-dependent activation of the transcription factor TIF-IA links rRNA synthesis to nutrient availability. *Genes Dev* **18**, 423-434 (2004).

94. Laplante, M. & Sabatini, D.M. An emerging role of mTOR in lipid biosynthesis. *Curr Biol* **19**, R1046-1052 (2009).

95. Duvel, K.*, et al.* Activation of a metabolic gene regulatory network downstream of mTOR complex 1. *Mol Cell* **39**, 171-183 (2010).

96. Li, S., Brown, M.S. & Goldstein, J.L. Bifurcation of insulin signaling pathway in rat liver: mTORC1 required for stimulation of lipogenesis, but not inhibition of gluconeogenesis. *Proc Natl Acad Sci U S A* **107**, 3441-3446 (2010).

97. Brugarolas, J.B., Vazquez, F., Reddy, A., Sellers, W.R. & Kaelin, W.G., Jr. TSC2 regulates VEGF through mTOR-dependent and -independent pathways. *Cancer Cell* **4**, 147-158 (2003).

98. Phung, T.L.*, et al.* Pathological angiogenesis is induced by sustained Akt signaling and inhibited by rapamycin. *Cancer Cell* **10**, 159-170 (2006).

99. Sarbassov, D.D.*, et al.* Prolonged rapamycin treatment inhibits mTORC2 assembly and Akt/PKB. *Mol Cell* **22**, 159-168 (2006).

100. Guertin, D.A.*, et al.* Ablation in mice of the mTORC components raptor, rictor, or mLST8 reveals that mTORC2 is required for signaling to Akt-FOXO and PKCalpha, but not S6K1. *Dev Cell* **11**, 859-871 (2006).

101. Jacinto, E.*, et al.* SIN1/MIP1 maintains rictor-mTOR complex integrity and regulates Akt phosphorylation and substrate specificity. *Cell* **127**, 125-137 (2006).

102. Sarbassov, D.D.*, et al.* Rictor, a novel binding partner of mTOR, defines a rapamycin-insensitive and raptor-independent pathway that regulates the cytoskeleton. *Curr Biol* **14**, 1296-1302 (2004).

103. Lee, J.Y.*, et al.* mTOR activation induces tumor suppressors that inhibit leukemogenesis and deplete hematopoietic stem cells after Pten deletion. *Cell Stem Cell* **7**, 593-605 (2010).

104. Kalaitzidis, D.*, et al.* mTOR complex 1 plays critical roles in hematopoiesis and Pten-loss-evoked leukemogenesis. *Cell Stem Cell* **11**, 429-439 (2012).

105. Chen, C.*, et al.* TSC-mTOR maintains quiescence and function of hematopoietic stem cells by repressing mitochondrial biogenesis and reactive oxygen species. *J Exp Med* **205**, 2397-2408 (2008).

106. Huang, J., Nguyen-McCarty, M., Hexner, E.O., Danet-Desnoyers, G. & Klein, P.S. Maintenance of hematopoietic stem cells through regulation of Wnt and mTOR pathways. *Nat Med* **18**, 1778-1785 (2012).

107. Chen, C., Liu, Y., Liu, Y. & Zheng, P. mTOR regulation and therapeutic rejuvenation of aging hematopoietic stem cells. *Sci Signal* **2**, ra75 (2009).

108. Zheng, L.*, et al.* Biological pathway selection through Bayesian integrative modeling. *Stat Appl Genet Mol Biol* **13**, 435-457 (2014).

109. Goodell, M.A. Introduction: Focus on hematology. CD34(+) or CD34(-): does it really matter? *Blood* **94**, 2545-2547 (1999).

110. Seita, J.*, et al.* Gene Expression Commons: an open platform for absolute gene expression profiling. *PLoS One* **7**, e40321 (2012).

111. Rayess, H., Wang, M.B. & Srivatsan, E.S. Cellular senescence and tumor suppressor gene p16. *Int J Cancer* **130**, 1715-1725 (2012).

112. Cancelas, J.A.*, et al.* Rac GTPases differentially integrate signals regulating hematopoietic stem cell localization. *Nat Med* **11**, 886-891 (2005).

113. Olson, M.F., Ashworth, A. & Hall, A. An essential role for Rho, Rac, and Cdc42 GTPases in cell cycle progression through G1. *Science* **269**, 1270-1272 (1995).

114. Zegers, M. Roles of P21-activated kinases and associated proteins in epithelial wound healing. *Int Rev Cell Mol Biol* **267**, 253-298 (2008).

115. Smith, F.M., *et al.* Mice with a disruption of the imprinted Grb10 gene exhibit altered body composition, glucose homeostasis, and insulin signaling during postnatal life. *Mol Cell Biol* **27**, 5871-5886 (2007).

116. Cao, X.R., *et al.* Nedd4 controls animal growth by regulating IGF-1 signaling. *Sci Signal* **1**, ra5 (2008).

117. Liu, M., *et al.* Grb10 promotes lipolysis and thermogenesis by phosphorylation-dependent feedback inhibition of mTORC1. *Cell Metab* **19**, 967-980 (2014).

118. Jahn, T., Seipel, P., Urschel, S., Peschel, C. & Duyster, J. Role for the adaptor protein Grb10 in the activation of Akt. *Mol Cell Biol* **22**, 979-991 (2002).

119. Logue, J.S. & Morrison, D.K. Complexity in the signaling network: insights from the use of targeted inhibitors in cancer therapy. *Genes Dev* **26**, 641-650 (2012).

120. Hoekstra, E.J., *et al.* Lmx1a is an activator of Rgs4 and Grb10 and is responsible for the correct specification of rostral and medial mdDA neurons. *Eur J Neurosci* **37**, 23-32 (2013).

121. Shalaby, F., *et al.* Failure of blood-island formation and vasculogenesis in Flk-1-deficient mice. *Nature* **376**, 62-66 (1995).

122. Poulos, M.G., *et al.* Endothelial Jagged-1 is necessary for homeostatic and regenerative hematopoiesis. *Cell Rep* **4**, 1022-1034 (2013).

123. Brenet, F., Kermani, P., Spektor, R., Rafii, S. & Scandura, J.M. TGFbeta restores hematopoietic homeostasis after myelosuppressive chemotherapy. *J Exp Med* **210**, 623-639 (2013).

124. Fonseca-Pereira, D., *et al.* The neurotrophic factor receptor RET drives haematopoietic stem cell survival and function. *Nature* **514**, 98-101 (2014).

125. Tycko, B. & Morison, I.M. Physiological functions of imprinted genes. *J Cell Physiol* **192**, 245-258 (2002).

126. Zou, P.*, et al.* p57(Kip2) and p27(Kip1) cooperate to maintain hematopoietic stem cell quiescence through interactions with Hsc70. *Cell Stem Cell* **9**, 247-261 (2011).

127. Kubota, Y., Osawa, M., Jakt, L.M., Yoshikawa, K. & Nishikawa, S. Necdin restricts proliferation of hematopoietic stem cells during hematopoietic regeneration. *Blood* **114**, 4383-4392 (2009).

128. Morrison, M.M.*, et al.* mTOR Directs Breast Morphogenesis through the PKC-alpha-Rac1 Signaling Axis. *PLoS Genet* **11**, e1005291 (2015).

129. Aslan, J.E., Tormoen, G.W., Loren, C.P., Pang, J. & McCarty, O.J. S6K1 and mTOR regulate Rac1-driven platelet activation and aggregation. *Blood* **118**, 3129-3136 (2011).

130. Rodgers, J.T.*, et al.* mTORC1 controls the adaptive transition of quiescent stem cells from G0 to G(Alert). *Nature* **510**, 393-396 (2014).

131. Yilmaz, O.H.*, et al.* Pten dependence distinguishes haematopoietic stem cells from leukaemia-initiating cells. *Nature* **441**, 475-482 (2006).

132. Gan, B. & DePinho, R.A. mTORC1 signaling governs hematopoietic stem cell quiescence. *Cell Cycle* **8**, 1003-1006 (2009).

133. Quinn, C.C., Pfeil, D.S. & Wadsworth, W.G. CED-10/Rac1 mediates axon guidance by regulating the asymmetric distribution of MIG-10/lamellipodin. *Curr Biol* **18**, 808-813 (2008).

134. Yu, Y.*, et al.* Phosphoproteomic analysis identifies Grb10 as an mTORC1 substrate that negatively regulates insulin signaling. *Science* **332**, 1322-1326 (2011).

135. Hsu, P.P.*, et al.* The mTOR-regulated phosphoproteome reveals a mechanism of mTORC1-mediated inhibition of growth factor signaling. *Science* **332**, 1317-1322 (2011).

136. Leibinger, M., Andreadaki, A. & Fischer, D. Role of mTOR in neuroprotection and axon regeneration after inflammatory stimulation. *Neurobiol Dis* **46**, 314-324 (2012).

137. Park, K.K., Liu, K., Hu, Y., Kanter, J.L. & He, Z. PTEN/mTOR and axon regeneration. *Exp Neurol* **223**, 45-50 (2010).

138. Park, K.K.*, et al.* Promoting axon regeneration in the adult CNS by modulation of the PTEN/mTOR pathway. *Science* **322**, 963-966 (2008).

139. Oury, F.*, et al.* Endocrine regulation of male fertility by the skeleton. *Cell* **144**, 796-809 (2011).

140. Lee, N.K.*, et al.* Endocrine regulation of energy metabolism by the skeleton. *Cell* **130**, 456-469 (2007).

141. Delany, A.M.*, et al.* Osteopenia and decreased bone formation in osteonectin-deficient mice. *J Clin Invest* **105**, 915-923 (2000).

142. Clark, C.J. & Sage, E.H. A prototypic matricellular protein in the tumor microenvironment--where there's SPARC, there's fire. *J Cell Biochem* **104**, 721-732 (2008).